tosis in U87-derived GSLCs. In this study, we demonstrated that VHL downregulated the tumorigenicity and self-renewal of U87-derived GSLCs by inhibiting the JAK/STAT signaling pathway and upregulated the expression of PTEN, which acted coordinately with VHL. We also analyzed the role of STAT3 in GSLCs and the possibility of therapy using VHL.

Materials and methods

Isolation of CD133+ U87-derived GSLCs. The human glioblastoma cell line U87MG was purchased from ATCC. U87MG is derived from a human glioblastoma and is widely used in biological studies on gliomas, particularly those examining the pathway involved in glioma proliferation. We initially cultured naive U87MG cells in Dulbecco's modified Eagle's medium (DMEM) containing 10% fetal calf serum (FCS) (Fig. 1A) which was, according to a previous study (4), subsequently changed to non-serum DMEM/F12 containing B27 supplement (Gibco-Invitrogen, Grand Island, NY, USA), basic FGF (PeproTech EC Ltd., Rocky Hill, NJ, USA) and EGF (Upstate Biotechnology, Lake Placid, NY, USA). CD133+ cells were then selected by using an autoMACS™ Pro Separator (Miltenyi Biotec, Bergisch Gladbach, Germany) and neurosphere-forming cells were cultured in the same medium (Fig. 1B). Serial passage of the cells was performed by a mechanical dissociation method and passaged cells, i.e., GSLCs, were used for subsequent experiments.

Characterization of U87-derived GSLCs. Characterization of U87 GSLCs was carried out by immunocytochemistry using the following antibodies: anti-CD133 (Santa Cruz Biotechnology, San Diego, CA, USA), anti-STAT3 (Cell Signaling Technology, Danvers, MA, USA), anti-JAK2 (Santa Cruz Biotechnology), anti-VHL (Santa Cruz Biotechnology), anti-Elongin A (Abgent, San Diego, CA, USA), anti-PTEN (Santa Cruz Biotechnology), anti-NeuroD (Santa Cruz Biotechnology), anti-MAP2 (Sigma-Aldrich, St. Louis, MO, USA) and anti-GFAP antibodies (Dako, Glostrup, Denmark), as described below. In addition, cell proliferation, tumorigenicity in the subcutaneous tissue of SCID mice (Charles River, Yokohama, Japan), as well as soft agar colony and neurosphere formation were examined as described below.

Influence of VHL on U87-derived GSLCs. We hypothesized that STAT3 was inhibited by VHL, since most BC-box family proteins, including VHL, have the ability to inhibit the JAK/STAT pathway. STAT3 plays a role in stem cell maintenance. Therefore, we investigated whether VHL was able to downregulate STAT3 in GSLCs. Initially, we constructed a VHL-expressing adenovirus vector, as previously described (15).

VHL-expressing adenovirus vector. The VHL-expressing adenovirus vector was prepared as previously described (15). Adenovirus vector encoding human VHL (VHL54-213 amino acids) was generated by the use of the cosmid vector pAxCAwt. As a control vector, the vector for green fluorescent protein (GFP), generated by the use of pAxCAwt, was obtained from the Riken Gene Bank (Saitama, Japan). For adenovirus infection, U87 GSCs were seeded into 6-cm dishes (1x10^6 cells/cm^2) 1 day prior to infection. The cells were then incubated for 1 h with 5 μl of the virus solution diluted to 1x10^7 plaque-forming
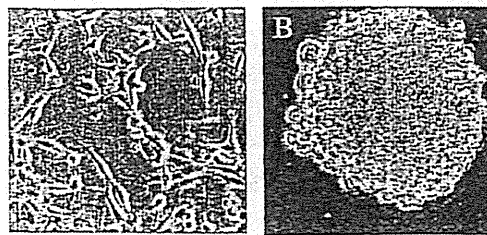

Figure 1. Morphology of cells. (A) Naive U87MG cells. (B) U87MG-derived glioma stem-like cells forming neurospheres.

units per milliliter in DMEM/F12 medium containing 5% FCS at a multiplicity of infection of 10, which is a condition sufficient for nearly 100% cell infection. VHL-expressing adenovirus vector was transferred to U87 GSLCs following dissociation of the neurospheres into single cells. Two days following the transfection in dishes, some of the cultured cells were transferred onto a cover glass and subsequently fixed for immunocytochemical study while the remaining were used to extract protein for western blot analysis.

Fluorescence-immunocytochemical study using confocal laser microscopy. Naive U87MG cells attached to round cover slips were fixed for 24 h with 10% formalin naturally deodorized buffer solution. After irrigating twice with phosphate-buffered saline (PBS), the fixed cells were blocked with 5% normal donkey serum for 30 min. Subsequently, primary antibodies (anti-NeuroD, anti-MAP2, anti-STAT3, anti-VHL, anti-PTEN, anti-JAK2 and anti-GFAP) were diluted with PBS (1:200) and incubated with the cells for 1 h at room temperature. Following irrigation 3 times with PBS, the cells were incubated in the dark for 45 min at room temperature with FITC-linked anti-mouse IgG antibody (Sigma-Aldrich) or TRIC-linked anti-rabbit IgG antibody (Sigma-Aldrich) as secondary antibodies. Following a further 3 irrigations with PBS, the cells were incubated for 5 min with DAPI (Molecular Probes, Eugene, OR, USA) diluted 1:3,000 with PBS. Finally, the cover glasses bearing the cells were placed on glass slides following application of ProLong Gold Antifade Reagent (Life Technologies, Grand Island, NY, USA) to the slides. The cells were then observed under an FV300 confocal microscope (Olympus, Tokyo). Cell nuclei appeared as red fluorescence and primary antibody-reactive antigens as green fluorescence.

Western blot analysis. Protein was extracted from the cells with RIPA buffer (Thermo Scientific, Rockford, IL, USA; 0.05 M Tris-HCl, pH 7.4, containing 0.15 M NaCl, 0.25% deoxycholic acid, 1% NP-40, 0.1% SDS, 1 mM EDTA, 1 mM PMSF, 1 mM sodium orthovanadate, 1 mM sodium fluoride, 1 μg/ml leupeptin and 1 μg/ml aprotinin). Extracted proteins were electrophoresed on 8-15% SDS-PAGE gels and then transferred to polyvinylidene difluoride (PVDF) membranes by using an iBlot™ Gel Transfer Device (Life Technologies) for 7 min. The blots were probed with primary and secondary antibodies by using a SNAP id Protein Detection system (Merck Millipore, Darmstadt, Germany). Immunoreactive bands were visualized by chemiluminescence with ECL Western Blotting Detection Reagents (GE Healthcare, Japan). Images were analyzed with LAS-1000 (Fujifilm, Tokyo, Japan) and the density of the bands

was determined by using Image Gauge software (Fujifilm). The following primary antibodies were used: anti-CD133 (Biorbyt, Cambridge, UK), anti-STAT3, anti-JAK2, anti-VHL and anti-PTEN. Horseradish peroxidase (HRP)-linked anti-rabbit IgG and HRP-linked anti-mouse IgG were used as the secondary antibodies.

Neurosphere formation assay. The neurosphere formation assay was performed as follows (16): neurosphere-forming U87 GSLCs were dissociated into single cells by continuous pipetting for 10 min. Following confirmation of their single-cell status and dilution up to 5 cells/ml, 200 µl of the cell solution was placed into each well of a 96-well plate (mean, one cell per well). Subsequently, neurospheres ≥50 µm in diameter in a single plate were counted under a phase-contrast microscope 1 week following placement of the cells.

Soft agar colony formation assay. This assay was performed as previously described (17). Briefly, following dissociation of the U87 GSLC neurospheres, a single-cell suspension (1,000 cells/ml) in 0.5 ml of 0.3% agar in a medium consisting of 10% FCS in DMEM/F12 was overlaid onto 0.5 ml of 0.6% agar medium in the wells of 24-well plates. Following 3 weeks of cultivation in a 5% CO_2 incubator, each well was examined under a stereoscopic microscope for colonies consisting of >40 cells.

Cell-proliferation assay. Cell proliferation was examined as previously described (18). After U87 GSLCs had been dissociated into single cells by 10-min continuous pipetting using a long thin pipette, the cells were transfected with the VHL-expressing adenovirus vector or GFP-expressing adenovirus vector as a control. They were then cultured in the U87 GSLC maintenance medium. Starting 1 day after the cultures had been prepared, the number of cells was counted as follows: control vector-transfected and VHL-expressing vector-transfected U87 GSLCs were washed once with PBS, then dissociated into single cells by 10-min continuous pipetting using a long thin pipette. The number of viable cells was counted following staining with trypan blue.

Implantation into SCID mice. Subcutaneous implantation of control- or VHL-transfectant U87 GSLCs (1×10^4 U87 GSLCs) into 4 SCID Hairless Outbred (SHO-Prkdc Hr) mice (Charles River) for each vector was performed. The mice were housed in a clean, temperature-controlled room on a 12-h day/night cycle with free access to food and water. One month following implantation, the mice were examined for subcutaneously-formed tumors. Formed tumors were histologically examined with hematoxylin-eosin staining and immunohistochemically with anti-CD133, anti-GFAP and anti-STAT3 antibodies. The animal experimental procedure was approved by the Institutional Animal Use Committee of Yokohama City University and was in accordance with the National Institutes of Health Guidelines for the care and use of laboratory animals.

Statistical analysis. Data were analyzed by ANOVA (SPSS II; SPSS, IBM, Tokyo, Japan) and a P-value of <0.05 was considered to indicate a statistically significant difference.
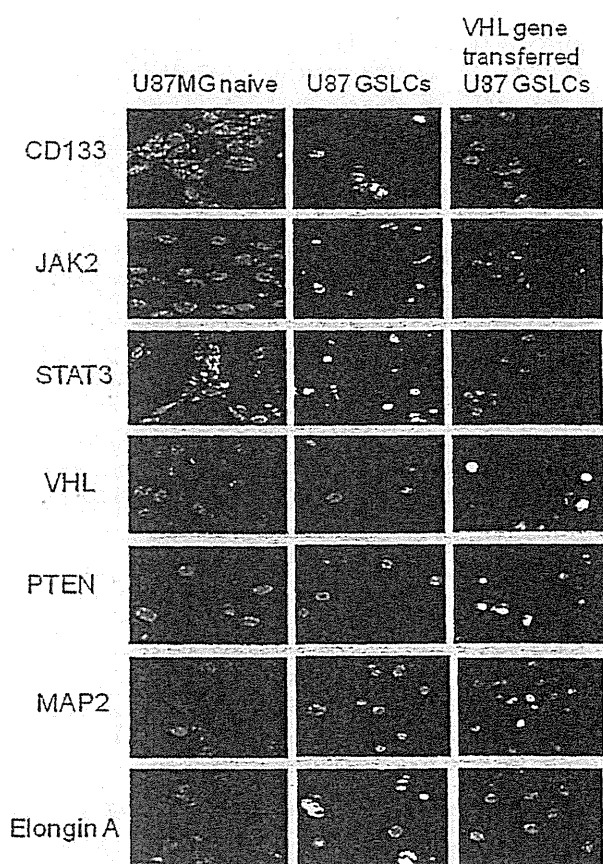

Figure 2. Fluorescence-immunocytochemical studies on U87MG naive cells, U87 glioma stem-like cells (GSLCs) and VHL-transfectant U87 GSLCs. Immunoreactivity toward primary antibodies is shown in green and DAPI-stained nuclei appears as red fluorescence.

Results

Immunocytochemical study on naive U87MG cells. Naive cells of the U87MG cell line were cultured as substrate-attached cells in DMEM containing 10% FCS and the cells were passaged every 4-5 days. The cells displayed 2 or 3 cellular processes and were Elongin A positive, rarely CD133 positive, VHL negative and MAP2 negative. Also, the majority of the cells were STAT3 positive, partially JAK1 positive and PTEN negative.

U87MG-derived GSLCs. To obtain GSLCs from the U87MG cell line, we changed the medium to non-serum DMEM containing basic FGF, EGF and B27 supplement. One month later, the cultured cells tended to float. By using the MACS method with anti-CD133 antibody, we collected CD133-positive fractioned cells, according to the manufacturer's instructions, and then cultured them in the above medium for 2-3 weeks. The cultured cells formed numerous floating neurospheres. The neurospheres were dissociated and some of the single cells were stained by fluorescence immunocytochemistry for characterization, whereas the remaining were used for soft agar colony and neurosphere formation, as well as for cell proliferation assays. In addition, protein was extracted from neurospheres for western blot analysis.
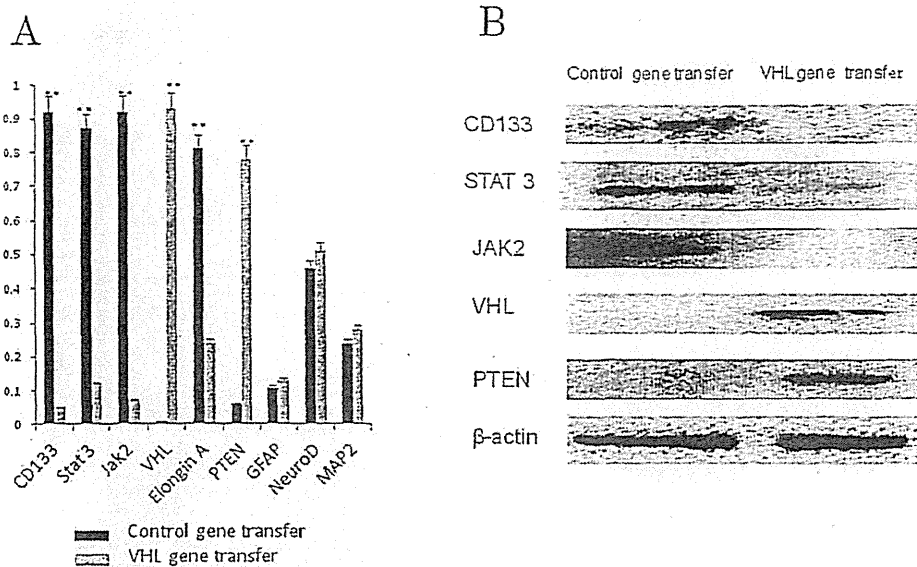
Figure 3. (A) Immunoreactivity rates for control-vector and VHL-vector glioma stem-like cell (GSLC) transfectants are shown. Expressions of CD133, STAT3, JAK2 and Elongin A were significantly inhibited, whereas those of VHL and PTEN were significantly increased in VHL-transfectant GSLCs compared to the control cells. Expressions of GFAP, NeuroD and MAP2 were not significantly altered. $P<0.05$, $P<0.01$. (B) Western blot analysis of control-vector and VHL-vector GSLC transfectants. Control-vector GSLC transfectants expressed CD133, STAT3 and JAK2, whereas VHL-vector GSLC transfectants expressed VHL and PTEN, but exhibited inhibited expression of CD133, STAT3 and PTEN. β-actin expression was equal in both cells.

Fluorescence-immunocytochemical study on U87 GSLCs. Results of the immunocytochemical analysis of U87 GSLCs are depicted in Figs. 2 and 3A. The percentage of CD133-positive cells as well as STAT3- and JAK2-positive cells was higher in the control-vector than in the VHL-vector transfectants. The majority of the naive U87 cells were Elongin A positive, as were the U87 GCLSs. U87 GSLCs were also VHL and PTEN negative, similar to U87 naive cells. Approximately half of those cells were NeuroD positive, of which some were GFAP positive.

Western blot analysis. The results of western blot analysis (Fig. 3B) supported the immunocytochemical data. U87 GSLCs expressed CD133, STAT3 and JAK2, but not VHL or PTEN. Expression of CD133, STAT3 and JAK1 was not detected following VHL gene transfer, contrary to VHL and PTEN expression, which was detected. Following VHL gene transfer to U87 GSLCs, the percentage of VHL and PTEN positive cells was increased, whereas that of CD133, STAT3 and JAK2 positive cells was decreased.

Soft agar colony formation, neurosphere formation and cell proliferation. The results of the colony-formation assay in soft agar medium demonstrated significantly greater colony formation in the control vector-transfected compared to the VHL-expressing vector-transfected U87 GSLCs (P<0.001) (Fig. 4A). Neurosphere formation, which is a reflection of the self-renewal ability, was also significantly greater in the former than in the latter (P<0.001) (Fig. 4B). Proliferation of control vector-transfected U87 GSLCs was significantly more pronounced compared to the VHL gene-transfected GSLCs 7 days following transfection (P<0.01) (Fig. 4C), although the difference between them was smaller than in the case of the soft agar colony or neurosphere formation assay.

Implantation of U87 GSLCs into SCID mice. Although subcutaneous transplantation of U87 GSLCs into SCID mice always resulted in tumor formation, transplantation of VHL gene-transfected U87 GSLCs resulted in markedly reduced or no tumor formation. The tumors arising from the U87 GSLCs transplanted into the SCID mice exhibited the pathological features of glioblastoma and most of the cells in the tumor tissue were CD133- and STAT3- positive but showed no immunoreactivity indicative of GFAP (Fig. 5).

Discussion

Glioma cancer stem cells are defined by their self-renewal ability, CD133-positivity, and transplantation ability in SCID mice (3). U87 GSLCs constructed by us exhibited these properties and may thus be considered a subpopulation of naive U87 cells. U87 GSLCs may be cultured in non-serum medium containing growth factors such as basic FGF and EGF. Glioma cancer stem cells are also known as glioma-initiating cells. GSLCs possess various mechanisms related to treatment tolerability, epigenetics and PTEN/PI3K/Akt signaling (19), and they reside in a hypoxic niche (14). Our results suggest that U87 GSLCs had a high capacity for colony and neurosphere formation. VHL inhibited STAT3, JAK2 and Elongin A. In addition, VHL upregulated PTEN expression. However, GFAP, NeuroD and MAP2 levels were not significantly affected by the VHL gene transfer. These results suggest that VHL affected the JAK/STAT pathway as well as the PTEN/PI3K/Akt pathway; they also suggest that upregulation of PTEN by VHL gene transfer may affect the PI3K/Akt pathway, since PTEN is a PI3K/Akt pathway inhibitor (19). STAT3 has been reported to play an important role in the self-renewal ability of cancer stem cells. VHL inhibited the implantation ability, as well as soft agar colony and neurosphere formation, all of which are
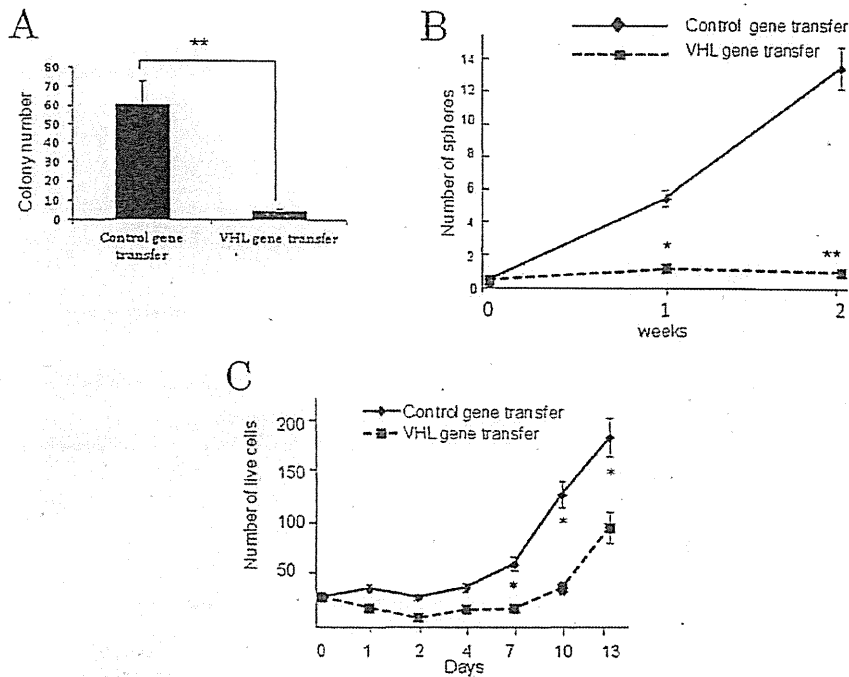
Figure 4. (A) Results on soft agar colony formation by control-vector and VHL-vector GSLC transfectants. Colony formation by the VHL transfectants was significantly inhibited. (B) Results for neurosphere formation. After one week, soft agar colony formation of VHL gene-transfected GSLCs was significantly inhibited. (C) Results of cell-proliferation assay. After 7 days, control gene-transfected GSLCs showed significantly greater proliferation than the VHL gene-transfected GSLCs (P<0.01). *P<0.01, **P<0.001.
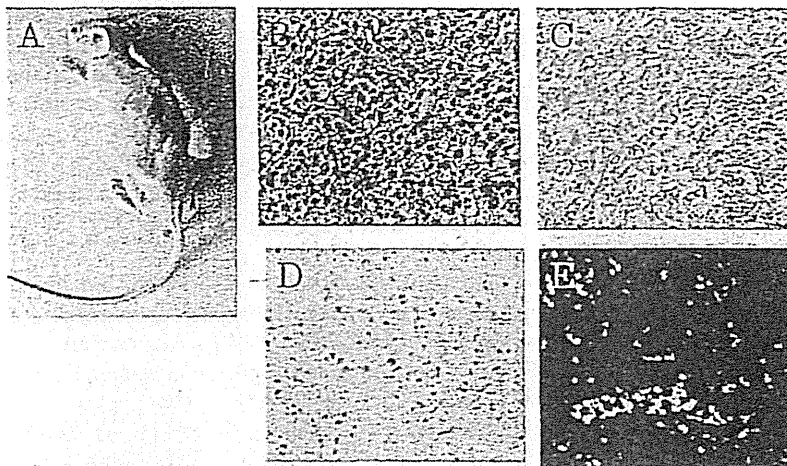

Figure 5. (A) Subcutaneously implanted GSLCs in the SCID mouse (red arrow). (B) Hematoxylin-eosin staining of subcutaneously implanted GSCs. Histologically, the appearance was similar to human glioblastomas. (C) Immunostaining by the Avidin-Biotin Complex (ABC) method for the detection of STAT3. Cytoplasm of most cells shows immunoreactivity toward anti-STAT3 antibody. Counter-staining with hematoxylin. (D) Immunostaining by the ABC method for examination of GFAP expression. Only few cells are immunoreactive with anti-GFAP antibody. Counter-staining with hematoxylin. (E) Fluorescence immunostaining for detection of CD133 expression. The majority of the cells are immunopositive for CD133 (green). Nuclei are stained with DAPI (light blue).

key characteristics of cancer stem cells. Our results suggest that these characteristics may be related to the JAK/STAT or PTEN/PI3K/Akt pathways in GSLCs. VHL inhibits HIF-1α under normoxic, but not under hypoxic, conditions by acting through the ubiquitin/proteasome system (20). Although *VHL* gene mutations are not frequently found in gliomas (21), function of the *VHL* gene is maintained under normoxic, but not

hypoxic, conditions (20). In addition, overexpression of VHL inhibits tumorigenesis and reduces the proliferation of glioma cells (22). The core of glioblastomas is reported to be in the hypoxic state and glioblastomas are characterized by their necrotic regions due to poor vascularization, which leads to inadequate blood supply and, consequently, to hypoxic and necrotic areas (23). It is suggested that GSLCs are maintained

in vivo in a niche characterized by reduced oxygen tension, i.e., in a hypoxic niche (13). U87-derived GCLSs exhibited negative expression of the VHL protein and, thus, the use of U87 GCLSs may be considered adequate for characterization of GCLSs. Overexpression of VHL upregulated PTEN and downregulated the JAK/STAT pathway, although it did not significantly affect the expression of neuronal differentiation markers such as NeuroD, GFAP and MAP2. In addition, overexpression of VHL significantly downregulated the proliferation of U87 GSLCs. However, the overexpression of VHL inhibited cell proliferation of U87 GSLCs to a lesser extent than it did soft agar colony and neurosphere formation, or implantation capacity into SCID mice. These results suggest that VHL inhibited the tumorigenicity and self-renewal ability via the JAK/STAT pathway and also affected the PTEN/PI3K/Akt pathway, both of which are critical in GSLCs, but it did not affect the differentiation of the GSLCs.

In conclusion, VHL overexpression downregulated the tumorigenicity and self-renewal ability in U87 GCLSs via the JAK/STAT pathway and upregulated PTEN. VHL overexpression therapy may be promising for the regulation of GSLCs under hypoxic conditions.

Acknowledgements

References

1. Stupp R, Mason WP, van den Bent MJ, *et al*: Radiotherapy plus concomitant and adjuvant temozolomide for glioblastoma. N Engl J Med 352: 987-996, 2005.
2. Friedman HS, Prados MD, Wen PY, *et al*: Bevacizumab alone and in combination with irinotecan in recurrent glioblastoma. J Clin Oncol 27: 4733-4740, 2009.
3. Singh SK, Hawkins C, Clarke ID, Squire JA, Bayani J, Hide T, Henkelman RM, Cusimano MD and Dirks PB: Identification of human brain tumour initiating cells. Nature 432: 396-401, 2004.
4. Yu SC, Ping YF, Yi L, Zhou ZH, Chen JH, Yao XH, Gao L, Wang JM and Bian XW: Isolation and characterization of cancer stem cells from a human glioblastoma cell line U87. Cancer Lett 265: 124-134, 2008.
5. Sherry MM, Reeves A, Wu JK and Cochran BH: STAT3 is required for proliferation and maintenance of multipotency in glioblastoma stem cells. Stem Cells 27: 2383-2392, 2009.
6. Villalva C, Martin-Lannerée S, Cortes U, Dkhissi F, Wager M, Le Corf A, Tourani JM, Dusanter-Fourt I, Turhan AG and Karayan-Tapon L: STAT3 is essential for the maintenance of neurosphere-initiating tumor cells in patients with glioblastomas: a potential for targeted therapy? Int J Cancer 128: 826-838, 2011.
7. Yang YP, Chang YL, Huang PI, *et al*: Resveratrol suppresses tumorigenicity and enhances radiosensitivity in primary glioblastoma tumor initiating cells by inhibiting the STAT3 axis. J Cell Physiol 227: 976-993, 2012.
8. Ohno M, Natsume A, Kondo Y, Iwamizu H, Motomura K, Toda H, Ito M, Kato T and Wakabayashi T: The modulation of microRNAs by type I IFN through the activation of signal transducers and activators of transcription 3 in human glioma. Mol Cancer Res 7: 2022-2030, 2009.
9. Ivanov SV, Salnikow K, Ivanova AV, Bai L and Lerman MI: Hypoxic repression of STAT1 and its downstream genes by a pVHL/HIF-1 target DEC1/STRA13. Oncogene 26: 802-812, 2007.
10. Kamura T, Sato S, Haque D, Liu L, Kaelin WG Jr, Conaway RC and Conaway JW: The Elongin BC complex interacts with the conserved SOCS-box motif present in members of the SOCS, ras, WD-40 repeat, and ankyrin repeat families. Genes Dev 12: 3872-3881, 1998.
11. Dasari VR, Kaur K, Velpula KK, Gujrati M, Fassett D, Klopfenstein JD, Dinh DH and Rao JS: Upregulation of PTEN in glioma cells by cord blood mesenchymal stem cells inhibits migration via downregulation of the PI3K/Akt pathway. PLoS One 5: e10350, 2010.
12. Frew IJ, Thoma CR, Georgiev S, Minola A, Hitz M, Montani M, Moch H and Krek W: pVHL and PTEN tumour suppressor proteins cooperatively suppress kidney cyst formation. EMBO J 27: 1747-1757, 2008.
13. Bar EE: Glioblastoma, cancer stem cells and hypoxia. Brain Pathol 21: 119-129, 2011.
14. Qiu B, Sun X, Zhang D, Wang Y, Tao J and Ou S: TRAIL and paclitaxel synergize to kill U87 cells and U87-derived stem-like cells in vitro. Int J Mol Sci 13: 9142-9156, 2012.
15. Yamada H, Dezawa M, Shimazu S, Baba M, Sawada H, Kuroiwa Y, Yamamoto I and Kanno H: Transfer of the von Hippel-Lindau tumor suppressor gene to neuronal progenitor cells in treatment for Parkinson's disease. Ann Neurol 54: 352-359, 2003.
16. Hägerstrand D, He X, Bradic Lindh M, Hoefs S, Hesselager G, Ostman A and Nistér M: Identification of a SOX2-dependent subset of tumor- and sphere-forming glioblastoma cells with a distinct tyrosine kinase inhibitor sensitivity profile. Neuro Oncol 13: 1178-1191, 2011.
17. Kanno H, Kuwabara T, Shinonaga M, Chang CC, Tanaka Y, Sugio Y, Morita H, Yasumitsu H, Umeda M and Nagashima Y: Establishment of a human glioma cell line bearing a homogeneously staining chromosomal region and releasing α- and β-type transforming growth factors. Acta Neuropathol 79: 30-36, 1989.
18. Yamada S, Kanno H and Kawahara N: Trans-membrane peptide therapy for malignant glioma by use of a peptide derived from the MDM2 binding site of p53. J Neurooncol 109: 7-14, 2012.
19. Bleau AM, Hambardzumyan D, Ozawa T, Fomchenko EI, Huse JT, Brennan CW and Holland EC: PTEN/PI3K/Akt pathway regulates the side population phenotype and ABCG2 activity in glioma tumor stem-like cells. Cell Stem Cell 4: 226-235, 2009.
20. Maxwell PH, Wiesener MS, Chang GW, Clifford SC, Vaux EC, Cockman ME, Wykoff CC, Pugh CW, Maher ER and Ratcliffe PJ: The tumour suppressor protein VHL targets hypoxia-inducible factors for oxygen-dependent proteolysis. Nature 399: 271-275, 1999.
21. Kanno H, Shuin T, Kondo K, Yamamoto I, Ito S, Shinonaga M, Yoshida M and Yao M: Somatic mutations of the von Hippel-Lindau tumor suppressor gene and loss of heterozygosity on chromosome 3p in human glial tumors. Cancer Res 57: 1035-1038, 1997.
22. Sun X, Liu M, Wei Y, Liu F, Zhi X, Xu R and Krissansen GW: Overexpression of von Hippel-Lindau tumor suppressor protein and antisense HIF-1alpha eradicates gliomas. Cancer Gene Ther 13: 428-435, 2006.
23. Valk PE, Mathis CA, Prados MD, Gilbert JC and Budinger TF: Hypoxia in human gliomas: demonstration by PET with fluorine-18-fluoromisonidazole. J Nucl Med 33: 2133-2137, 1992.

A hypoxia-inducible factor (HIF)-3α splicing variant, HIF-3α4 impairs angiogenesis in hypervascular malignant meningiomas with epigenetically silenced HIF-3α4

Hitoshi Ando [a,b], Atsushi Natsume [a,*], Kenichiro Iwami [a], Fumiharu Ohka [a], Takahiro Kuchimaru [c], Shinae Kizaka-Kondoh [c], Kengo Ito [d], Kiyoshi Saito [b], Sachi Sugita [e], Tsuneyoshi Hoshino [e], Toshihiko Wakabayashi [a]

[a] Department of Neurosurgery, Nagoya University School of Medicine, Nagoya, Japan
[b] Department of Neurosurgery, Fukushima Medical University School of Medicine, Fukushima, Japan
[c] Department of Biomolecular Engineering, Tokyo Institute of Technology Graduate School of Bioscience and Biotechnology, Yokohama, Japan
[d] National Center for Geriatrics and Gerontology, Aichi, Japan
[e] MICRON Inc.Medical Facilities Support Department, Aichi, Japan

ARTICLE INFO

ABSTRACT

Hypoxia inducible factor is a dominant regulator of adaptive cellular responses to hypoxia and controls the expression of a large number of genes regulating angiogenesis as well as metabolism, cell survival, apoptosis, and other cellular functions in an oxygen level-dependent manner. When a neoplasm is able to induce angiogenesis, tumor progression occurs more rapidly because of the nutrients provided by the neovasculature. Meningioma is one of the most hypervascular brain tumors, making anti-angiogenic therapy an attractive novel therapy for these tumors. HIF-3α has been conventionally regarded as a dominant-negative regulator of HIF-1α, and although alternative HIF-3α splicing variants are extensively reported, their specific functions have not yet been determined. In this study, we found that the transcription of HIF-3α4 was silenced by the promoter DNA methylation in meningiomas, and inducible HIF-3α4 impaired angiogenesis, proliferation, and metabolism/oxidation in hypervascular meningiomas. Thus, HIF-3α4 could be a potential molecular target in meningiomas.

© 2013 Elsevier Inc. All rights reserved.

1. Introduction

Brain tumors are classified into grades I–IV by the World Health Organization (WHO) according to histological features, with grade I being the most benign and grade IV being the most severe. Meningiomas are frequent neoplasms accounting for approximately 25% of all intracranial tumors [11]. They are mainly characterized by a benign histology and an indolent clinical course, and most are pathologically diagnosed as WHO grade I and curable by surgical resection. However, grade II or III meningiomas are occasionally encountered. Even more troublesome, some populations of meningiomas with benign pathological findings (WHO grade I) pursue a malignant course [12–14]. Our group has previously reported the use of whole genome methylation analysis to predict which tumors will undergo this malignant clinical course, and we were able to predict the outcome in meningioma patients

on the basis of the methylation status of 5 hub genes, including HIF-3α [15].

When a neoplasm is able to induce angiogenesis, tumor progression occurs more rapidly because of the nutrients provided by the neovasculature [1–3]. Meningioma is one of the most hypervascular tumors, making anti-angiogenic therapy an attractive novel therapy for these tumors [16]. This therapy targets angiogenetic factors, including vascular endothelial growth factor (VEGF) and platelet-derived growth factor, both of which are regulated by hypoxia inducible factor (HIF) [4,17,18].

HIF is a dominant regulator of adaptive cellular responses to hypoxia and controls the expression of a large number of genes regulating angiogenesis as well as metabolism, cell survival, apoptosis, and other cellular functions in an oxygen level-dependent manner. HIF forms a dimer consisting of an unstable α subunit (HIF-α) and a stable β subunit (HIF-β). This dimer binds to specific sequences termed hypoxia response elements (HRE) in the promoter region of HIF target genes such as VEGF. There are 3 principal isoforms of the HIF-α subunit (HIF-1α, 2α, 3α). HIF-1α and HIF-2α share a similar domain architecture and undergo similar proteolytic regulation [4–6,10,17,19,20]. HIF-3α, on the other hand, has been

* Corresponding author. Address: Department of Neurosurgery, Nagoya University School of Medicine, 65 Tsurumai-cho, Showa-ku, Nagoya 466-8550, Japan. Fax: +81 52 744 2360.

E-mail address: anatsume@med.nagoya-u.ac.jp (A. Natsume).

conventionally regarded as a dominant-negative regulator of HIF-1α [4–10], and although alternative HIF-3α splicing variants are extensively reported, their specific functions have not yet been determined [5,7,8,10,21]. HIF-3α4, one of the HIF-3α splicing variants, is similar to mouse inhibitory Per/Arnt/Sim domain protein (IPAS). IPAS expression in hepatoma cells selectively impairs tumor vascular density, and inhibition of IPAS expression induces vascular growth in the cornea of mice [9].

In this study, we constructed a meningioma cell line stably expressing HIF-3α4 in order to elucidate the function of HIF-3α4 in hypervascular malignant meningioma. We addressed multiple novel functions of HIF-3α4 in hypervascular meningiomas; angiogenesis, proliferation, and metabolism/oxidation. HIF-3α4 could be a potential molecular target in meningiomas.

2. Materials and methods

2.1. Cell lines

The human meningioma cell lines IOMM-Lee and HKBMM were kindly provided by Drs. Anita Lai (University of California at San Francisco, CA) and Shinichi Miyatake (Osaka Medical University, Osaka, Japan), respectively. All cell lines were maintained in Dulbecco's modified Eagle medium (DMEM) containing 10% fetal bovine serum (FBS) and 1% penicillin/streptomycin. Cell lines were grown at 37 °C in a humidified atmosphere of 5% CO_2 under normoxic (20% O_2) or hypoxic (1% O_2) conditions.

2.2. Genetically engineered meningioma cells

Using the following protocol, we designed IOMM-Lee or HKBMM meningioma cell lines stably expressing green fluorescence protein (GFP) or GFP-tagged HIF-3α4, designated IO-GFP, IO-HIF3α4, HK-GFP, and HK-HIF3α4, respectively. pQCXIP-HIF3α4-GFP plasmid was prepared by the following protocol: HIF-3α transcript variant 3, isoform c complete cDNA (accession No. BC080551) was obtained from GeneCopoeia (Rockville, MD). This cDNA was amplified using the forward primer 5'-CTAGATGAATTCATGGCGCTGGGGCTG-CAGCG-3', including an EcoRI site and the reverse primer 5'-CTA-GATCGCGGCCGCTCAGCTCAGCAAGGTGTGGATGC-3', including a NotI site. Oligonucleotides were obtained from Greiner Japan (Tokyo, Japan). After amplification, the products were purified by a QIAquick® Spin kit (QIAGEN, Hilden, Germany) and sequenced on an automated DNA sequencer (ABI PRISM 310, Applied Biosystems, Foster City, CA). Then, the products were digested by EcoRI and NotI (Takara Bio, Otsu, Japan), and the DNA was inserted to pQCXIP retrovirus vector (Clontech, Mountain View, CA) that had previously been altered to contain the GFP gene by using the DNA Ligation kit (Takara Bio, Otsu, Japan). These plasmids were co-transfected with pVSV-G (Clontech) into the retroviral packaging cell line 293T using Lipofectamine 2000 reagent (Invitrogen, Carlsbad, CA) to produce retrovirus. At 24 h post-transfection with pQCXIP-HIF3α4-GFP and pVSV-G, the medium was changed to DMEM. After another 24 h, the supernatant containing viral particles was collected and filtered through a 0.45-μm-pore PVDF membrane filter (Millex®-HV Syringe Driven Filter Unit; Millipore, Bradford, MA). IOMM-Lee or HKBMM meningioma cells were incubated for 48 h with the viral supernatant plus 4 μg/mL polybrene infection/transfection reagent (Millipore). Cells were then treated with 10 μg/mL puromycin (Sigma–Aldrich, St. Louis, MO) for 1 week to select the cells stably expressing HIF-3α4 and GFP.

2.3. Demethylation treatment

Cells (1 × 10^5 cells) were seeded in 6-well plate and incubated for 24 h, then treated with 5-aza-2'-deoxycytidine at the final concentration of 0, 1 or 5 μM. After the first administration, the same dose agent was added four times in total every 12 h. At 12 h after the fourth administration, medium was changed, and cells then were collected and RNA was extracted.

2.4. RNA extraction, reverse transcriptase PCR, and quantitative real-time PCR

RNA was extracted from IOMM-Lee or HKBMM cell line using Trizol® (Invitrogen, Carlsbad, CA). The following gene-specific oligonucleotide primers were obtained from Greiner Japan: HIF-1α forward 5'-GAGCTTGCTCATCAGTTGCC-3' and reverse 5'-CTGTA CTGTCCTGTGGTGAC-3', and HIF-3α4 forward 5'-CCCAGAGCTCA-GAGGACGAG-3' and reverse 5'-CCCAACACACCAGGCTGAGA-3'. First-strand cDNA was synthesized by Transcriptor First Strand cDNA synthesis kit (Roche, Indianapolis, IN) according to the manufacturer's instructions. The resulting products were analyzed on a 2% agarose gel stained with ethidium bromide. Quantitative real-time PCR (qPCR) was performed using the LightCycler 480 system (Roche Applied Science, Mannheim, Germany) and the Light Cycler 480 SYBR Green I Master (Roche).

2.5. Antibodies

Anti-HIF-1α antibody and anti-HIF-3α antibody were obtained from Novus Biologicals (Littleton, CO). Anti-GFP antibody was from MBL (Nagoya, Japan). Anti-β-actin antibody was from Sigma–Aldrich.

2.6. Protein extracts and western blot analysis

Meningioma cell lysates were prepared by lysing cells in 200 μL of 2× lysis buffer (20% [v/v] glycerol, 13.5% [v/v] 1 M Tris–HCl, 40% [v/v] 10% SDS, 4.0 ng bromophenol blue, 10% [v/v] mercaptoethanol, 16.5% [v/v] water). Lysates (10 μL) were loaded into 10% Mini-PROTEAN TGX Gels (BIO-RAD, Hercules, CA). Separated proteins were electrotransferred onto PVDF membranes (Hybond-P, GE Healthcare, Buckinghamshire, United Kingdom); then, western blots were performed using the antibodies listed above. Bands were detected using ECL Western Blotting Detection Reagents (GE Healthcare).

2.7. Protein interaction assay

Meningioma cells were seeded in 10-cm cell culture dishes and lysed in TNE buffer (150 mM NaCl, 35 mM Tris–HCl, 1% NP-40, 1 mM EDTA, 10 μg/mL aprotinin) at 4 °C. The lysates were immunoprecipitated with the anti-GFP antibody bound to Pierce® Protein G Agarose (Thermo Scientific, Rockford, IL) according to the manufacturer's instructions. The immunoprecipitated samples were analyzed by western blotting as described above.

2.8. Wound scratch assay

Meningioma cells were seeded in 10-cm tissue culture dishes at a concentration of 30 × 10^4 cells/mL and cultured under normoxia or hypoxia. Linear wounds were generated in the monolayer with the tips of a sterile 200-μL plastic pipette. Cellular debris was removed by washing with phosphate buffered saline (PBS). PBS was removed, and DMEM supplemented with 2% [v/v] FBS and 1% [v/v] penicillin–streptomycin was added to the culture dishes. Every 6 h, wounds were photographed at 20 scratched points per dish and each wound area was estimated using Image J software (Rasband, W.S., Image J, National Institutes of Health, Bethesda, MD, http://rsb.info.nih.gov/ij/, 1997–2009).

2.9. Cell growth assay

Cells were seeded in 96-well plates at 1×10^3 cells/well. At 24 and 48 h after plating, the cells were treated using the Cell counting Kit-8 (Dojindo, Kumamoto, Japan), and the absorbance was examined by Multi Label Reader 2030 ARVO X4 (Perkin Elmer, Waltham, MA).

2.10. Quantification of tumor vessels and overall survival time

All animal experiments were conducted in accordance with the Faculty of medicine of Nagoya University. IO-GFP or IO-HIF3α4 cells, 3×10^5 cells/2 μL were stereotactically injected into the brain of Balb-c nu/nu nude mice (female, 5 weeks of age) under anesthesia using a Hamilton syringe (Hamilton, Reno, NV). The coordination was 1.4 mm posterior from bregma, 3.0 mm to the right, at a 4.0-mm depth from brain surface. The overall survival was measured for up to 40 days. Five minutes before the mice were euthanized, animals were perfused with 0.5 mL of 10 g/L 155 kDa tetramethylrhodamine isothiocyanate-dextran (tetramethylrhodamine) (Sigma–Aldrich). Tumor-bearing brains were rapidly removed and fixed in 4% paraformaldehyde at 4 °C for 24 h. Coronal sections (100 μm thick) were cut on a vibratome, and the samples were examined by a laser scanning confocal microscope (FV1000-D; Olympus, Tokyo, Japan). The vessels that were enhanced by tetramethylrhodamine in the region of interest (ROI) in the tumor were visible by the presence of green fluorescence from GFP, and these areas were scanned in a 521×521 pixel format in the x–y direction of the ROI using a ×10 frame scan and 16 optical sections along the Z-axis with a 50-μm step. After collecting the data from the vessels from 10 ROIs, the data were imported as binary and reconstructed to three-dimensional images. The number of vascular voxels per total voxels of the ROI was calculated. The processing was performed using Image J software.

2.11. Positron emission computerized-tomography (PET) imaging

Meningioma IO-GFP or IO-HIF3α4 cells (1×10^6 in 100 μL PBS) were injected subcutaneously into the left shoulder of Balb-c nu/nu nude mice (female, 5 weeks of age) under anesthesia. When the tumor size reached about 100 mm^3, PET examination was performed as follows: After 24 h fasting, 20 MBq/200 μL fluorodeoxyglucose (FDG) was intravenously injected under inhalational anesthesia. PET imaging was performed 60 min after this treatment, and accumulation of FDG was measured for 30 min. After 48 h FDG-PET examination, 7.5 MBq/200 μL fluoromisonidazole (FMISO) was administered to mice. After 90 min of free movement, inhalational anesthesia was introduced, and the accumulation of FMISO was measured for 30 min.

2.12. Statistical analysis

Data are expressed as mean ± SEM. Comparison of treatments against controls was made using one-way ANOVA followed by Fisher's LSD post hoc test using SPSS version 19 (IBM, Chicago, IL). P values of <0.05 were considered significant. The duration of overall survival were analyzed in the Kaplan–Meier format using the log-rank test for statistical significance.

3. Results

3.1. Hypoxia induces the expression of HIF-3α4

We previously demonstrated that HIF-3α4 was a DNA-methylated gene useful in predicting the outcome of meningiomas. As predicted, the expression of HIF-3α4 was not detected in untreated meningioma cell lines. By contrast, IOMM-Lee cell line expressed similarly high amounts of HIF-1α under normoxic and hypoxic conditions (Fig. 1A). A DNA-demethylating agent, 5-aza-2'-deoxycytidine, induced the expression of HIF-3α4 (Fig. 1B), suggesting that the transcription of HIF-3α4 is silenced by DNA methylation under normal conditions.

HIF-3α4, one of the HIF-3α splicing variants, is similar to mouse IPAS. It was of great interest to investigate how overexpression of HIF-3α4 affects the interaction between HIF-1α and angiogenesis in hypervascular meningioma. Therefore, we successfully generated GFP-tagged stable transfectants expressing HIF-3α4 (Fig. 1C). The finding was also consistent with another genetically-engineered cell line, HK-HIF3α4 (data not shown).

3.2. HIF-3α4 binds to HIF-1α

Previous reports showed that HIF-3α4 forms an abortive transcriptional complex with HIF-1α and prevents the engagement of HIF-1 to the HREs located in the promoter/enhancer regions of hypoxia-inducible genes [4,17,18]. In this study, cell lysate from IOMM-Lee cells stably expressing GFP-tagged HIF-3α4 (IO-HIF-3α4) was immunoprecipitated with anti-GFP antibody and then subjected to western blotting with anti-HIF-1α antibodies. As shown in Fig. 1D, western blotting with anti-HIF-1α detected a band corresponding to 93-kDa HIF-1α in the immunoprecipitated lysate from IO-HIF-3α4 but not in that from the control IO-GFP lysate. Consistent with the previous reports, this experiment demonstrated that HIF-3α4 binds to HIF-1α in meningioma.

Next, we investigated whether HIF-3α4 enhanced the transcription of hypoxia-inducible genes. The transcription of VEGF was markedly suppressed in IO-HIF-3α4 cells compared to IO-GFP cells (Fig. 1E).

### 3.3. HIF-3α4 directly inhibits the proliferation and invasion of meningioma cells

The HIF family is multifactorial; it regulates angiogenesis, metabolism, proliferation, and invasion/metastasis [20]. However, little is known about the function of HIF-3α4 in tumor cells. Overexpression of HIF-3α4 significantly retarded cell proliferation under normoxia and hypoxia (Fig. 2A). In scratch wound healing assay, healing speed was slower in IO-HIF-3α4 cells than in IO-GFP ($P < 0.05$, Fig. 2B), suggesting that HIF-3α4 inhibits proliferation and invasion in meningioma cells.

3.4. HIF-3α4 reduces neovascularization and glucose metabolism in meningioma

In order to visualize neovasculature in meningioma growing in the brain of mice, mice with GFP-tagged meningiomas were injected with tetramethylrhodamine (TMR). TMR-stained hyperdense vessels were observed in GFP-expressing tumors (Fig. 3A). Sequential images along the Z-axis allowed us to create three-dimensional images (Fig. 3B). The number of vascular voxels per total voxels of the ROI was calculated in IO-HIF-3α4 and IO-GFP meningiomas (Fig. 3C). Vascular density was significantly reduced in IO-HIF-3α4 tumors compared to IO-GFP tumors.

FDG, an analog of glucose, was used to generate PET images representing glucose metabolic activity in a region of tumor tissue. In clinical settings, the FDG uptake of the tumor and reference region (the tumor-to-gray matter ratio; TGR) is relatively high in meningioma, and is correlated with the tumor aggressiveness determined by the MIB-1 index [11]. While FDG uptake was high in the control IO-GFP tumors, it was significantly reduced in IO-HIF-3α4 tumors (Fig. 3D). FMISO is a nitroimidazole derivative, and
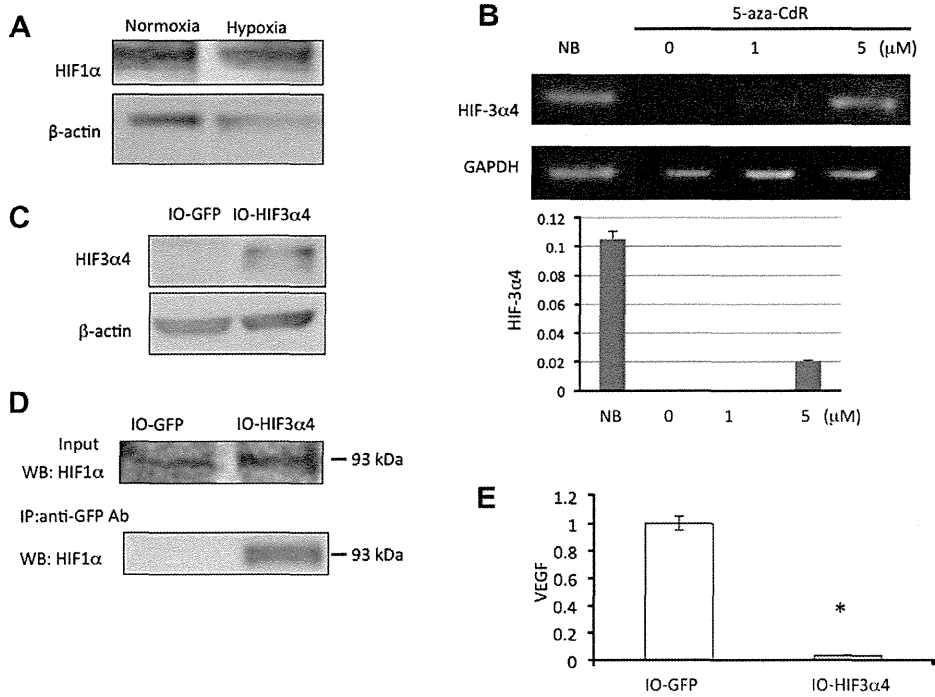
Fig. 1. (A) HIF-1α is constitutively expressed in IOMM-Lee meningioma cells under under normoxic and hypoxic conditions. (B) A DNA-demethylating agent, 5-aza-deoxycytidine (5-aza-CdR), induced the expression of HIF-3α4. (C) IOMM-Lee meningioma cells stably expressing GFP-tagged HIF-3α4 were generated through cloning and puromycin selection. (D) Lysates from IOMM-Lee cells stably expressing GFP or HIF-3α4 were immunoprecipitated using anti-HIF-1α antibody. We detected a band corresponding to 93-kDa HIF-1α in the immunoprecipitated lysate from IO-HIF-3α4, but not in that from the control IO-GFP. (E) The transcription of VEGF was markedly suppressed in IO-HIF-3α4 cells compared to IO-GFP cells.
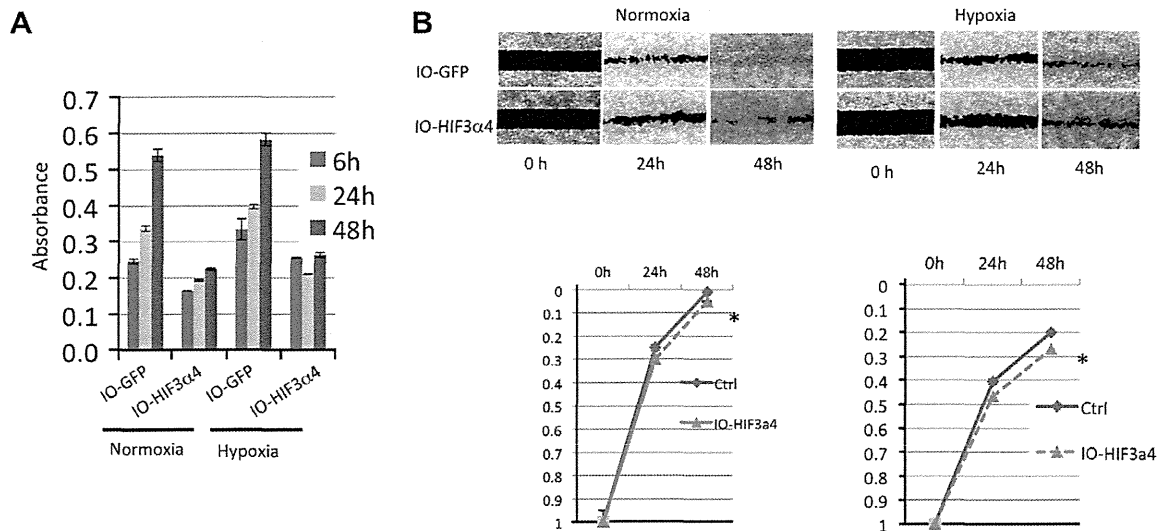
Fig. 2. HIF-3α4 directly inhibits the proliferation and invasion of meningioma cells. (A) Overexpression of HIF-3α4 significantly retarded cell proliferation under normoxia and hypoxia. (B) In scratch wound healing assay, the healing speed was slower in IO-HIF-3α4 cells than in IO-GFP cells ($P < 0.05$).

FMISO PET can image tumor hypoxia by increased FMISO tumor uptake, because FMISO metabolites are trapped exclusively by hypoxic cells [22]. In the control IO-GFP tumors, FMISO uptake was slightly higher than in the normal region. By contrast, HIF-3α4 overexpression markedly decreased FMISO uptake. As we discuss later, although HIF-3α4 reduced neovascularization (Fig. 3B), reduction of FMISO uptake in IO-HIF-3α4 tumors may have resulted from decreased tumor size, rather than HIF-3α4-mediated

hypoxia. Indeed, there was a tendency toward correlation between FMISO uptake and tumor volume.

3.5. HIF-3α4 prolongs the survival time of mice with malignant meningiomas

IO-GFP or IO-HIF-3α4 cells (3×10^5 cells) were inoculated into the brain of nude mice. The animals with IO-GFP control tumors
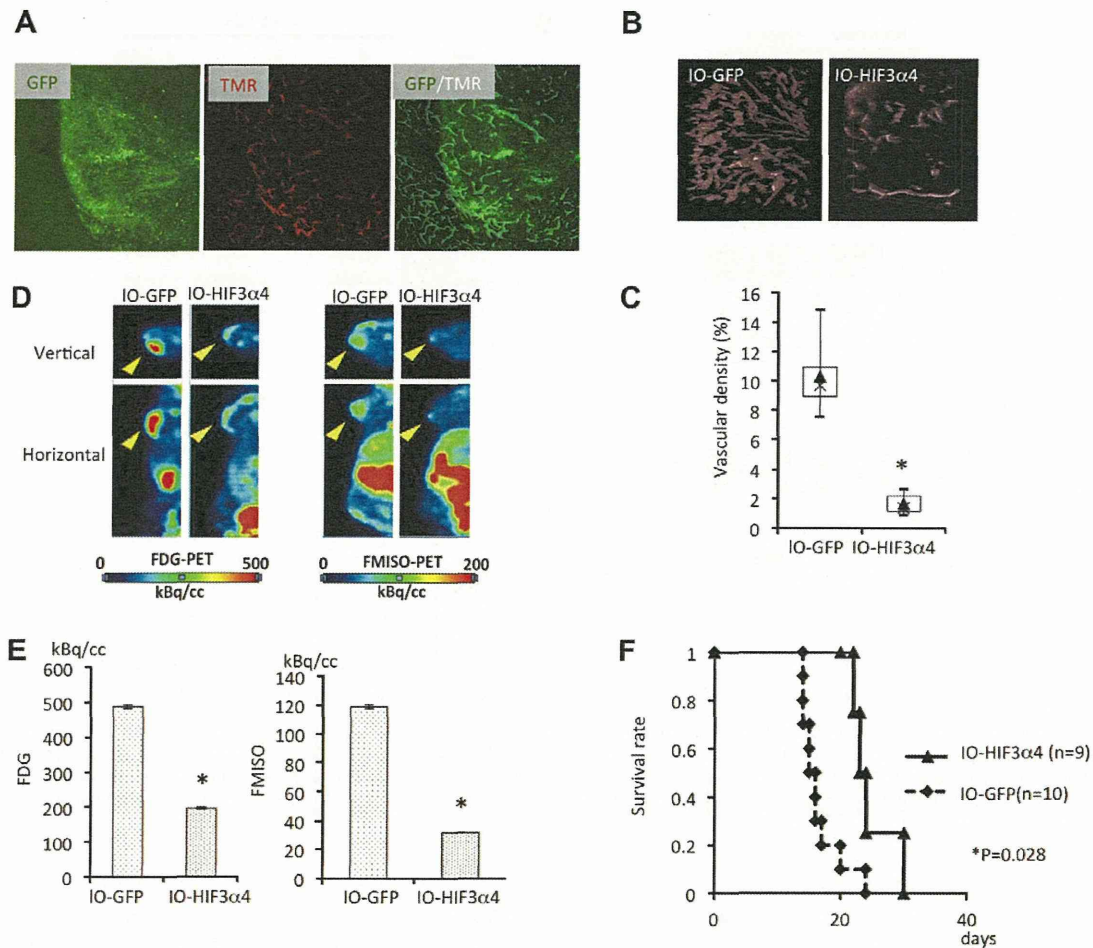
Fig. 3. HIF-3α4 reduced neovascularization and glucose metabolism in meningioma. (A) Tetramethylrhodamine (TMR)-stained hyper-dense vessels seen in GFP-expressing tumors. (B) Sequential images along the Z-axis enabled us to create three-dimensional images. (C) The number of vascular voxels per total voxels of the ROI was calculated in IO-HIF-3α4 and IO-GFP meningiomas. (D) FDG-PET (left) and FMISO-PET (right). While FDG uptake was extensively high in the control IO-GFP tumors, it was significantly reduced in IO-HIF-3α4 tumors. In the control IO-GFP tumors, FMISO uptake was slightly higher than the normal region. By contrast, overexpression of HIF-3α4 markedly decreased FMISO uptake.

died by 25 days after inoculation. However, the survival of mice with IO-HIF-3α4 tumors was prolonged significantly. This result suggests that the induction of HIF-3α4 was unable to cure mice with malignant meningiomas, but it did confer a survival advantage (Fig. 3F).

4. Discussion

First, the present study demonstrated that the HIF-1α expressed at considerable levels even under normoxic condition in IOMM-Lee meningioma cells. Taking into account that meningioma is one of the most hypervascular tumors, such levels of HIF-1α expression may be reasonable. The gene expression of endogenous HIF-3α4 appeared to be silenced probably due to DNA methylation [15]. Therefore the following experiments were performed under normoxia to assign a focus on the function of transfected HIF-3α4.

Previously, Heikkil et al. indicated that HIF-3α4 directly bound to HIF-1α to inhibit its transcriptional activity [10]. In the present study, we confirmed the interaction between GFP tagged HIF-3α4 and HIF-1α in IO-HIF3α4 cells by immunoprecipitation assay (Fig. 1D). Next we addressed the effect of HIF-3α4 on proliferation, invasion, angiogenesis, glucose-metabolism, and hypoxic state by cell growth assay, wound scratch assay, vascular imagings, FDG-PET, and FMISO-PET, respectively. As the results, all of these activities were decreased in IO-HIF3α4 cells (Figs. 2 and 3). As Rankin and Giaccia, and Semenza et al. reported, the expression of various genes such as VEGF, GLUT-1, EPO, E-CADHERIN and others, relevant to angiogenesis, metabolism, proliferation and invasion/metastasis, are regulated by HIF-1α [4,6,7,10,17,20,23]. Also, as mentioned above, I confirmed the interaction between HIF-1α and HIF-3α4 and the suppression of VEGF expression in IO-HIF3α4 cells. These results together suggest that overexpression of HIF-3α4 might inhibit transcription activity of HIF-1α. Since HIF-1α has many other target genes, their functions should also be examined in future. To clarify the function of HIF-3α4, studies using the knock down system for HIF-3α4 would also be required.

Energy in the tumor is produced by a high rate of glycolysis followed by lactic acid fermentation in the cytosol, rather than by a low rate of glycolysis followed by oxidation of pyruvate (Warburg effect), leading to high FDG uptake [24,25]. High FDG/FMISO-uptake in IO-GFP cells tumor (Fig. 3D and E) might be due to constitutive transcriptional activity of HIF-1α, leading to high rate tumor growth and thus high demands for glucose and oxygen. By contrast, IO-HIF3α4 cells tumor grew slower than IO-GFP cells tumor, possibly resulted in lower demand for glucose and oxygen. Thus

FDG and FMISO uptake in IO-HIF3α4 cells kept at low levels. It is very likely that this difference in tumor growth rate caused the difference in overall survival time in the mouse xenograft model (Fig. 3F). From these results, the association between the expression of HIF-3α4 and vascular density or tumor growth in clinical meningioma samples should be examined in future.

In conclusion, present study suggested that overexpression of HIF-3α4 might suppress tumor activities of the meningioma cell line. Although further studies are required, strategies to express high levels of HIF-3α4 could possibly contribute to establish a new treatment for malignant meningiomas.

References

[1] J.Y. Kim, Y.G. Cha, S.W. Cho, E.J. Kim, M.J. Lee, J.M. Lee, J. Cai, H. Ohshima, H.S. Jung, Inhibition of apoptosis in early tooth development alters tooth shape and size, J. Dent. Res. 85 (2006) 530–535.
[2] O. Warburg, On the origin of cancer cells, Science 123 (1956) 309–314.
[3] M. Preusser, M. Hassler, P. Birner, M. Rudas, T. Acker, K. Plate, G. Widhalm, E. Knosp, H. Breitschopf, J. Berger, Microvascularization and expression of VEGF and its receptors in recurring meningiomas: pathobiological data in favor of anti-angiogenic therapy approaches, Clin. Neuropathol. 31 (2012) 352–360.
[4] A. Weidemann, R. Johnson, Biology of HIF-1α, Cell Death Differ. 15 (2008) 621–627.
[5] M.A. Maynard, Human HIF-3 4 is a dominant-negative regulator of HIF-1 and is down-regulated in renal cell carcinoma, FASEB J. 19 (2005) 1396–1406.
[6] T. Tanaka, M. Wiesener, W. Bernhardt, K.U. Eckardt, C. Warnecke, The humanHIF(hypoxia-inducible factor)-3α gene is a HIF-1 target gene and may modulate hypoxic gene induction, Biochem. J. 424 (2009) 143–151.
[7] A. Pasanen, M. Heikkilä, K. Rautavuoma, M. Hirsilä, K.I. Kivirikko, J. Myllyharju, Hypoxia-inducible factor (HIF)-3α is subject to extensive alternative splicing in human tissues and cancer cells and is regulated by HIF-1 but not HIF-2, Int. J. Biochem. Cell Biol. 42 (2010) 1189–1200.
[8] Y. Makino, Inhibitory PAS domain protein (IPAS) is a hypoxia-inducible splicing variant of the hypoxia-inducible factor-3alpha locus, J. Biol. Chem. 277 (2002) 32405–32408.
[9] Y. Makino, R. Cao, K. Svensson, G. Bertilsson, M. Asman, H. Tanaka, Y. Cao, A. Berkenstam, L. Poellinger, Inhibitory PAS domain protein is a negative regulator of hypoxia-inducible gene expression, Nature 414 (2001) 550–554.
[10] M. Heikkil, A. Pasanen, K.I. Kivirikko, J. Myllyharju, Roles of the human hypoxia-inducible factor (HIF)-3f¿ variants in the hypoxia response, Cell. Mol. Life Sci. (2011) 1–17.
[11] J.W. Lee, K.W. Kang, S.H. Park, S.M. Lee, J.C. Paeng, J.K. Chung, M.C. Lee, D.S. Lee, 18F-FDG PET in the assessment of tumor grade and prediction of tumor recurrence in intracranial meningioma, Eur. J. Nucl. Med. Mol. Imaging 36 (2009) 1574–1582.
[12] H. Maier, D. Öfner, A. Hittmair, K. Kitz, H. Budka, Classic, atypical, and anaplastic meningioma: three histopathological subtypes of clinical relevance, J. Neurosurg. 77 (1992) 616–623.
[13] T. Backer-Grøndahl, B.H. Moen, S.H. Torp, The histopathological spectrum of human meningiomas, Int. J. Clin. Exp. Pathol. 5 (2012) 231.
[14] M.K. Aghi, B.S. Carter, G.R. Cosgrove, R.G. Ojemann, S. Amin-Hanjani, R.L. Martuza, W.T. Curry Jr, F.G. Barker, Long-term recurrence rates of atypical meningiomas after gross total resection with or without postoperative adjuvant radiation, Neurosurgery 64 (2009) 56–60.
[15] Y. Kishida, A. Natsume, Y. Kondo, I. Takeuchi, B. An, Y. Okamoto, K. Shinjo, K. Saito, H. Ando, F. Ohka, Epigenetic subclassification of meningiomas based on genome-wide DNA methylation analyses, Carcinogenesis 33 (2012) 436–441.
[16] P.Y. Wen, J. Drappatz, Novel therapies for meningiomas, Expert Rev. Neurother. 6 (2006) 1447–1464.
[17] G.L. Semenza, HIF-1: upstream and downstream of cancer metabolism, Curr. Opin. Genet. Dev. 20 (2010) 51–56.
[18] W.G. Kaelin Jr, P.J. Ratcliffe, Oxygen sensing by metazoans: the central role of the HIF hydroxylase pathway, Mol. Cell 30 (2008) 393–402.
[19] P. Maxwell, G. Dachs, J. Gleadle, L. Nicholls, A. Harris, I. Stratford, O. Hankinson, C. Pugh, P. Ratcliffe, Hypoxia-inducible factor-1 modulates gene expression in solid tumors and influences both angiogenesis and tumor growth, Proc. Natl. Acad. Sci. 94 (1997) 8104.
[20] E. Rankin, A. Giaccia, The role of hypoxia-inducible factors in tumorigenesis, Cell Death Differ. 15 (2008) 678–685.
[21] M.A. Maynard, Multiple splice variants of the human HIF-3alpha locus are targets of the von Hippel–Lindau E3 ubiquitin ligase complex, J. Biol. Chem. 278 (2003) 11032–11040.
[22] G.F. Whitmore, A.J. Varghese, The biological properties of reduced nitroheterocyclics and possible underlying biochemical mechanisms, Biochem. Pharmacol. 35 (1986) 97–103.
[23] D. Bo, S. Laijun, S. Hongwei, Expression of HIF-1, COX-2 and the correlation with angiogenesis in meningioma, Chin. J. Pract. Nerv. Dis. 2 (2008) 005.
[24] J.W. Kim, C.V. Dang, Cancer's molecular sweet tooth and the Warburg effect, Cancer Res. 66 (2006) 8927–8930.
[25] V. Barresi, G. Tuccari, Evaluation of neo-angiogenesis in a case of chordoid meningioma, J. Neurooncol. 95 (2009) 445–447.

VHL 病に伴う中枢神経系血管芽腫

中村　英夫[1]，倉津　純一[1]，執印　太郎[2]

1）熊本大学大学院生命科学研究部脳神経外科，2）高知大学医学部泌尿器科

Craniospinal Hemangioblastoma associated with Von Hippel-Lindau Disease Review

Hideo Nakamura, M.D.[1], Junichi Kuratsu, M.D.[1], and Taro Shuuin, M.D.[2]

1) Department of Neurosurgery, Graduate School of Life Sciences, Kumamoto University, 2) Departement of Urology, Kochi Medical School

Von Hippel-Lindau（VHL）disease is neoplastic syndrome that affects multiple organ systems. Most patients with this disease（60-80％）harbor hemangioblastomas and neurosurgeons often treat craniospinal hemangioblastomas in these patients. VHL disease is transmitted across generations in an autosomal dominant manner ; its incidence is 1 in 36,000. The VHL tumor suppressor gene is located on chromosome 3（3p25）and encodes for the VHL protein, which complexes with several proteins involved in the ubiquitin-dependent proteolysis of hypoxia-inducing factor（HIF）. The VHL protein appears to have several functionas and its dysregulation leads to angiogenesis and tumorigenesis. As most patients with VHL disease harbor central nervous system（CNS）hemangioblastomas, their management must be optimized to minimize morbidity and mortality. Although patients with VHL disease harbor not only CNS neoplasm but also cysts and/or neoplasms in other organs, in our study we reviewed the features of and the management strategies for only cranio-spinal hemangioblastomas in patients with VHL disease.

はじめに

Von Hippel-Lindau（VHL）病は神経線維腫症とともに脳神経外科医が治療に携わることが多い遺伝病である．常染色体優性遺伝の疾患で，複数の臓器に腫瘍性あるいは嚢胞性病変を多発する．1993 年に原因遺伝子（*VHL* 遺伝子）も同定され，その遺伝子産物における機能異常が全身のさまざまな腫瘍形成の原因となることが解明された．*VHL* 遺伝子は 3 番染色体短腕（3p25）に存在する腫瘍抑制遺伝子の一つであり，その遺伝子産物の機能異常が起こった場合，いかにしていろいろな腫瘍が形成されるかという分子生物学的機能に関しても解明されている．臨床的には，VHL 病は中枢神経系に血管芽腫が多発する疾患であり，脳神経外科医によって摘出されることが多い．しかし，VHL 病はあくまで全身性の疾患であり，中枢神経系以外の病態も十分に把握しながら診療すべき疾患である．今回，VHL 病に伴う中枢神経系血管芽腫について概説する．

連絡先：中村英夫，〒860-8556 熊本市本荘 1-1-1　熊本大学大学院生命科学研究部脳神経外科
Address reprint requests to：Hideo Nakamura, M.D., Department of Neurosurgery, Graduate School of Life Sciences, Kumamoto University, 1-1-1 Honjo, Kumamoto-shi, Kumamoto 860-8556, Japan

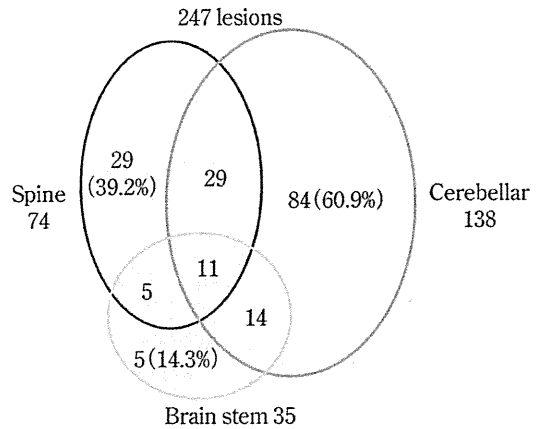|	Onset age	Frequency（%）
Total	33（9〜78）	60〜80
Cerebellar	33（9〜78）	44〜72
Brain stem	32（12〜46）	10〜25
Spine	33（12〜66）	40〜50
Supratentorial	34（unknown）	3〜6

from the report by Beitner MM（2011）and Lonser RR（2003）

Average：30.8 y.o.
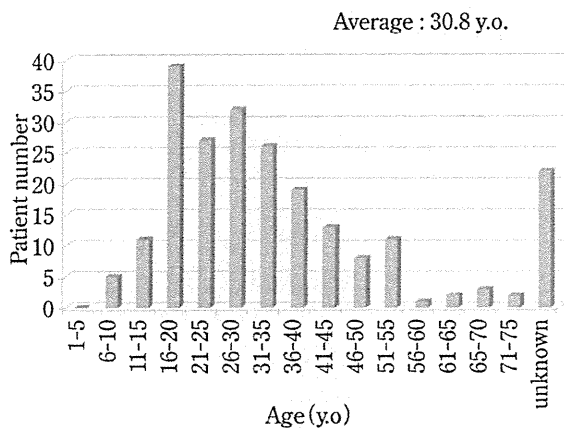
Fig. 1 Age distribution in patients with hemangioblastoma associated with VHL disease

Fig. 2 Craniospinal distribution of hemangioblastomas in patients with VHL

VHL 病に伴う中枢神経系腫瘍の 局在および発症年齢

VHL 病は常染色体優性の遺伝形式をとる浸透率 100％の疾患であり，発病率は 35,000〜40,000 人に 1 人 と推定されている．VHL 病の 60〜80％に中枢神経系疾 患を合併し，血管芽腫が 60〜80％，内耳リンパ嚢腫が 10〜15％認められる．VHL 病の平均寿命は 49 歳であり， 死因の 32％が腎癌，53％が血管芽腫といわれている[3]． 中枢神経系病変の頻度と発症年齢を Table1 に示すが，小 脳（44〜72％）に最も多く発生し，次いで脊髄（40〜 50％），脳幹（10〜25％）の順である．まれであるが大 脳半球，下垂体の発生例もある．平成 21 年度厚生労働 科学研究，難治性疾患克服研究事業研究奨励分野「フォ ン・ヒッペルリンドウ病の病態調査と診断治療系確立の 研究」班 国内病態調査結果（中間結果）による VHL 病 における中枢神経系血管芽腫の発症年齢の分布を Fig. 1 に示すが，平均発症年齢は 30.8 歳であった．小脳の血管 芽腫に関しては，多発性の場合，発症年齢が若く，1 個

の場合の発症年齢の平均が 30.8 歳に対して，2 個の場合 24.1 歳，3 個以上の場合も 24.1 歳であった．この結果を 踏まえて，調査班では VHL 関連血管芽腫（VHL-HB） の早期診断として VHL 病のハイリスク群の患者（遺伝 子検査陽性，家族歴がある，他臓器の発症で VHL 病が 疑われる）に対しては 11 歳から 2 年おきの脳，脊髄の 造影 MRI を撮影することを推奨している．中枢神経系血 管芽腫において VHL-HB は全体の 5〜30％の割合を占 め，平均 2.1 年ごとに新病巣が出現するという調査結果 であった．VHL 病ではない特発性の血管芽腫（S [sporadic]-HB）と VHL-HB と局在，発症年齢を比較す ると，VHL-HB は，S-HB と比較して発症年齢がおよそ 10 歳若く，また多発例が多く，さらに S-HB の局在が小 脳優位であることに対して，VHL-HB は，脳幹，脊髄に もできやすい[22]．本邦における調査班によりまとめられ た VHL-HB の 247 病変（小脳 138，脊髄 74，脳幹 35） の分布を Fig. 2 に示す．

症 状

中枢神経系の血管芽腫の症状は発生部位によるが，小 脳の場合には頭痛が最も多く（75％），歩行障害（55％）， 測定障害（29％），水頭症に伴う症状（28％），嘔気，嘔 吐（28％）と報告されている[8]．脳幹の場合は延髄（area postrema of the medulla）に好発し，延髄空洞症を合併す ることが多い（67％）[26]．脳幹の血管芽腫の多くは VHL 病を伴っており，孤発性の血管芽腫（S-HB）はまれで ある．Weil ら[24]は，感覚障害（55％），歩行障害（22％）， 嚥下障害（22％），反射亢進（22％），頭痛（11％）と報
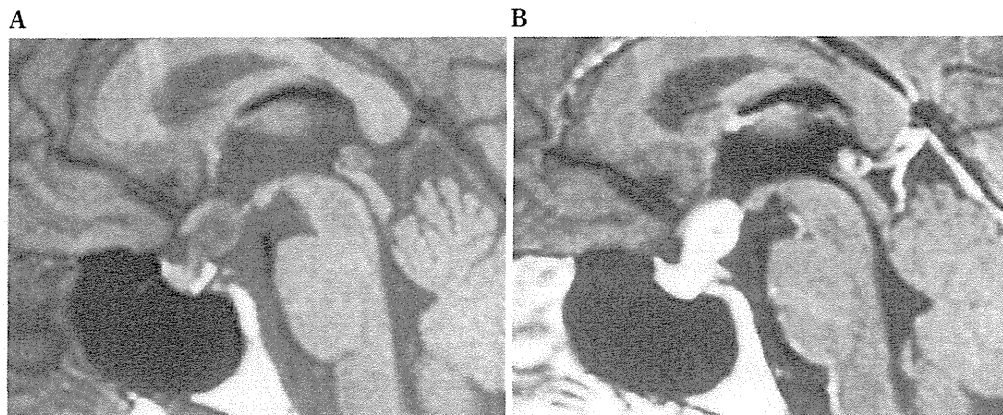
Fig. 3　Hemangioblastoma in pituitary
A：MRI T1-weighted image of hemangioblastoma associated with a cyst in the pituitary stalk.
B：The tumor is strongly enhanced with gadolinium-diethylenetriamine penta-acetic acid（Gd-DTPA）.

告している．脊髄も脳幹同様 VHL 病を伴っていることが多く，症状としては，感覚障害（83％），運動麻痺（65％），歩行障害（65％），反射亢進（52％），痛み（17％），失禁，失便（14％）との報告がある[22]．VHL 病に伴うテント上の血管芽腫に関しては 13 症例/18 病変の報告があるが[17]，側頭葉に好発している．また，囊胞を 6 病変（33％）で伴っており，6 症例が主に頭蓋内圧亢進症状，視野障害で発症している．VHL 病に伴い下垂体柄部に血管芽腫が発生するという報告も散見され[5]（Fig. 3），Lonser ら[11] の報告によると，250 例の VHL 病に伴う血管芽腫のうち 8 例（3％）であった．これはテント上の VHL-HB では最も多い 29％を占め，平均体積は 0.5±0.9 cm^3 であり，全例無症候性であった．また下垂体機能も正常のことが多く，治療の必要がなく経過観察でよいと結論づけている．

診　断

画像診断に関しては，MRI にて診断できる．囊胞を伴ってその中に壁在結節が存在するタイプ（Fig. 4A）と，囊胞を伴わず実質性のタイプ（Fig. 4B）があり，血管撮影においてはかなり高い vascularity が認められる（Fig. 4C）．MRI において基本的には T1 強調画像では低信号，T2 強調画像で高信号の腫瘍であり，MRI および CT アンギオグラフィーを併用することによって診断は容易である．VHL-HB では S-HB と比較して腫瘍周囲の浮腫や囊胞を伴いやすいという特徴がある．

病理診断に関しては，VHL-HB と S-HB においての

相違はまったくなく，World Health Organization（WHO）分類においては grade 1 の腫瘍である．HE 染色では，毛細管構造を示す豊富な血管網がこの腫瘍の基本構造となっており，polygodial stromal cell がこれらの豊富な血管の network に囲まれてグリア線維や microcyst と混在して存在する[25]（Fig. 5）．

鑑別診断としては angioblastic meningioma や VHL 病に合併しやすい腎癌の小脳転移と鑑別が困難な場合があるが，腎癌との鑑別には CD10，Inhibin，AE1/AE3，aquaporin1，Pax-2 の免疫染色が有用である[19)25]（Fig. 6）．また，血管芽腫が血流豊富なためか，血管芽腫に腎癌が転移した症例も報告されている[9]．

自然史

VHL に伴う中枢神経系の血管芽腫をどのようなタイミングで治療するか，またどのような間隔でフォローしていくかということを考慮するうえで，腫瘍の増大形式などの自然史は重要である．VHL に伴う血管芽腫に関する自然史の報告は散見されるが，Wanebo ら[23] が行った 160 例の連続した症例（655 病変の血管芽腫）の検討によると，腫瘍の増大を予見することは意外に困難である．彼らの結果によると，平均 51 カ月の観察期間で 34 症例（21.2％）に新病変が出現している．また増大形式に関しては 2 相性（増大期と静止期）のパターンをとるものもあれば，静止期がないものもあり，予想困難である．中には静止期の後の急激な増大形式（growth spurt）をとるものがあり，腫瘍細胞において *VHL* 遺伝子に加えてさ
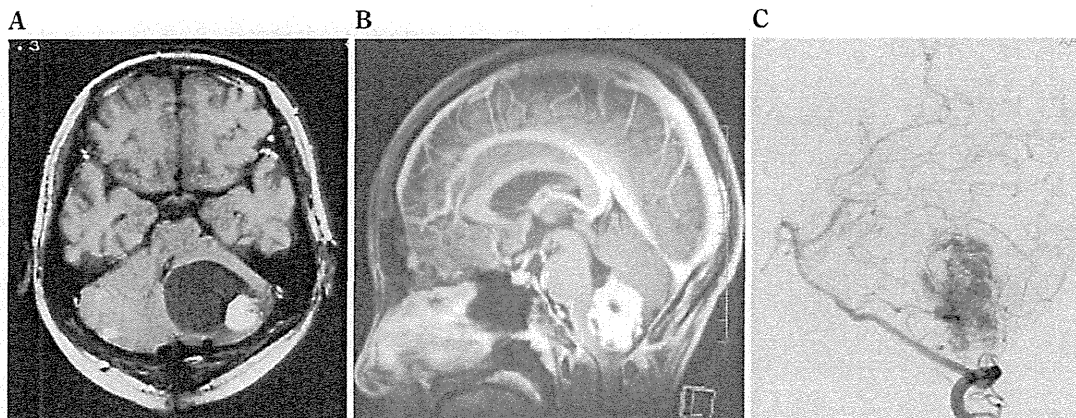
Fig. 4　Radiological imagings of hemangioblastomas
A：MRI of hemangioblastoma associated with a cyst locating at cerebellar hemisphere. Mural nodule is strongly enhanced with Gd-DTPA.
B：MRI of hemangioblastoma without cyst. Tumor is strongly enhanced with Gd-DTPA.
C：Angiography of B.
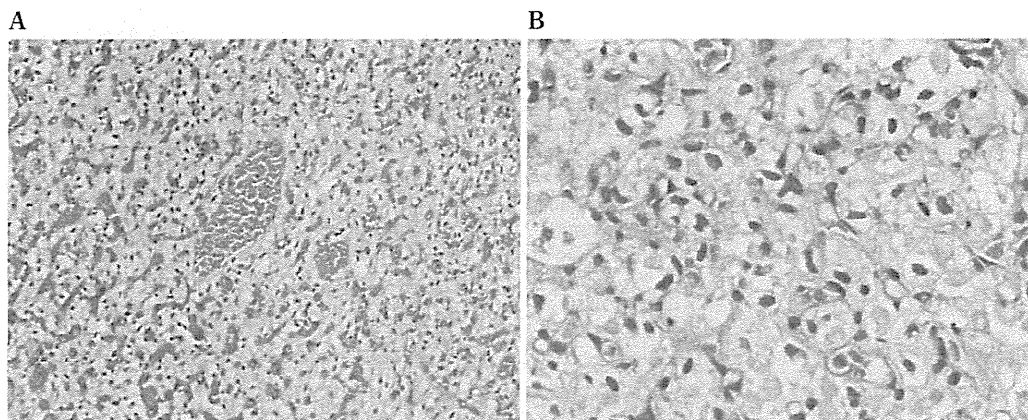
Fig. 5　Pathological findings of hemangioblastoma
A：Hematoxylin-Eosin（H-E）staining of hemangioblastoma（×10）showing a lot of vessels.
B：H-E staining of hemanigoblastoma（×40）showing stromal cells and microcysts.

らなる新しい遺伝子異常が起こった可能性がある．VHL病の多くの症例においては，増大期と静止期をもつことから，ホルモンなどの全身的な要素が腫瘍増大速度に影響している可能性があると考察されている．しかし，増大期，静止期の期間を推測することは非常に困難であり，フォローアップしている画像検査の期間にも左右されている．増大期が1回であるVHL患者のフォローアップ期間の平均は23±21カ月であり，2回であれば57±19カ月であり，静止期に関していえば，1回，2回，3回の静止期を観察しえたフォローアップ期間の平均はそれぞれ19±21，32±21，59±19カ月であった．つまり，長

くフォローできている患者ほど観察できた増大期，静止期の回数が多いという結果であった．彼らは，また増大予測因子として，囊胞の存在と症候性のものを挙げている．腫瘍に囊胞を伴う時，小脳では7倍，脳幹では15倍の速度で囊胞を伴わない腫瘍より速く増大していた．また症候性のものが無症候性のものより6～9倍速く増大する傾向にあった．同じグループであるが，Ammerman ら[1]は2006年に19症例のVHL病患者の143病変の血管芽腫を約12年フォローアップしているが，ほとんど全例増大するが（138病変，97％），約半分の病変（58病変，45％）しか発症しないという結果であった．
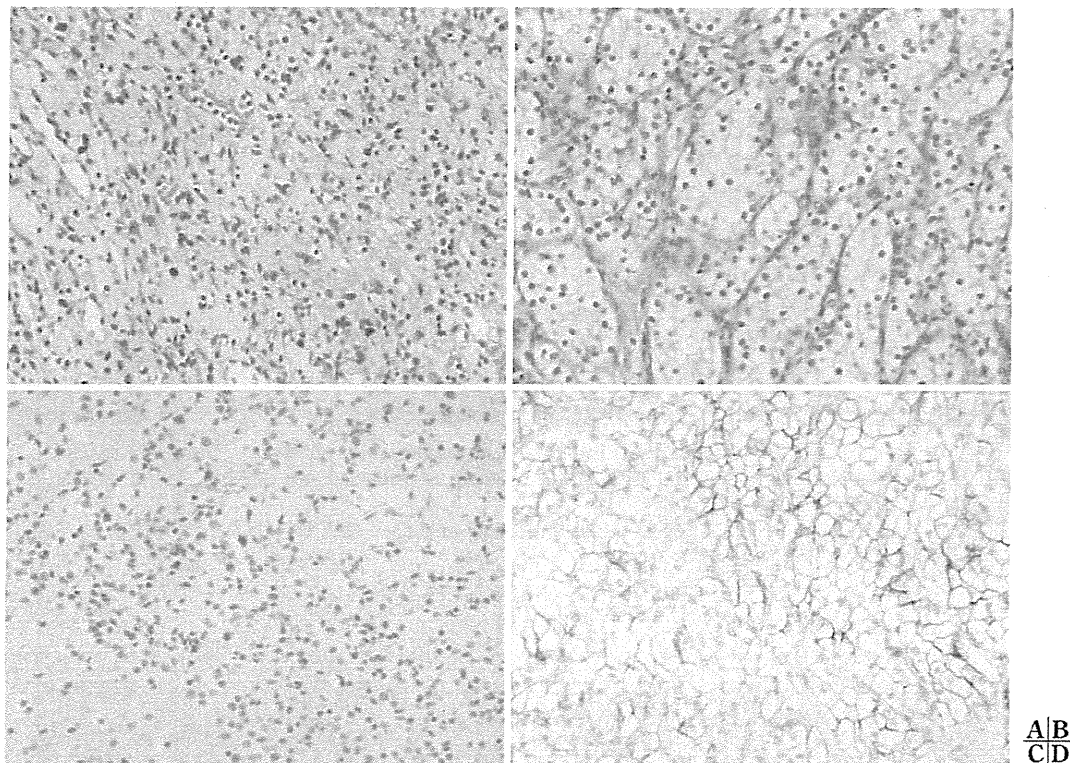
Fig. 6　Differential diagnosis between hemangioblastoma and renal carcinoma
　　　　A：H-E staining of hemangioblastoma.
　　　　B：H-E staining of renal carcinoma.
　　　　C：Immunohistochemical staining of inhibin for hemangioblastoma.
　　　　D：Immunohistochemical staining of inhibin for renal carcinoma.

VHL 病の血管芽腫においては度重なる治療を施行することが多い．少しでも腫瘍が増大した時に治療を開始するのではなく，症候性かどうか，腫瘍が増大し続けるのかどうかなど十分に見きわめることが重要である．

治療法

① 手　術

Lonser ら[12]によると VHL 病の血管芽腫に対して，症候性であること，発症前の切迫状態もしくは腫瘍が明らかな増大傾向を示している場合が適応である．彼らが手術を施行した VHL 病の血管芽腫の病変のうち症候性であったものは小脳で 37％，脳幹で 10％，脊髄で 50％であった．S-HB と VHL-HB の手術において何ら違いはないが，VHL 病においては中枢神経系以外の手術を施行されている場合があり，手術が度重なることが問題点として挙げられている．まず，小脳においては同じグループの Jagannathan ら[7]が 80 症例（126 手術，164 病変，

平均年齢：37.8 歳）の VHL 病に伴う血管芽腫の手術成績を報告している．症候性が 83％，無症候性が 17％であり，小脳における局在は半球 93％，虫部 7％であった（Fig. 7）．術後 3 カ月後の評価で 124 手術（98％）の症例で症候が改善もしくは安定していたという良好な成績であり，水頭症が合併していたものの改善率は 94％であった．また平均 61 カ月の長期フォローアップの結果再発はなかったと報告している．彼らは，小脳の血管芽腫の手術は安全であり効果的であり，水頭症を伴った症例でも腫瘍を完全に摘出できれば自然と軽快し，シャント等は必要ないと結論づけている[7]．次に脳幹の血管芽腫であるが，小脳より発生した腫瘍に比べて手術も困難である．Pavesi ら[16]の 14 例の報告では，3 例（複視，嚥下障害，手麻痺）に永続的な合併症がでている．ほとんどの症例で病変は背側に発生するために，比較的手術成績はよいと結論づけている報告もある[26]．Wind ら[26]が 44 症例（51 手術，71 病変）について術後 5.9±5 年フォローアップした結果を報告しているが，術直後の成績に
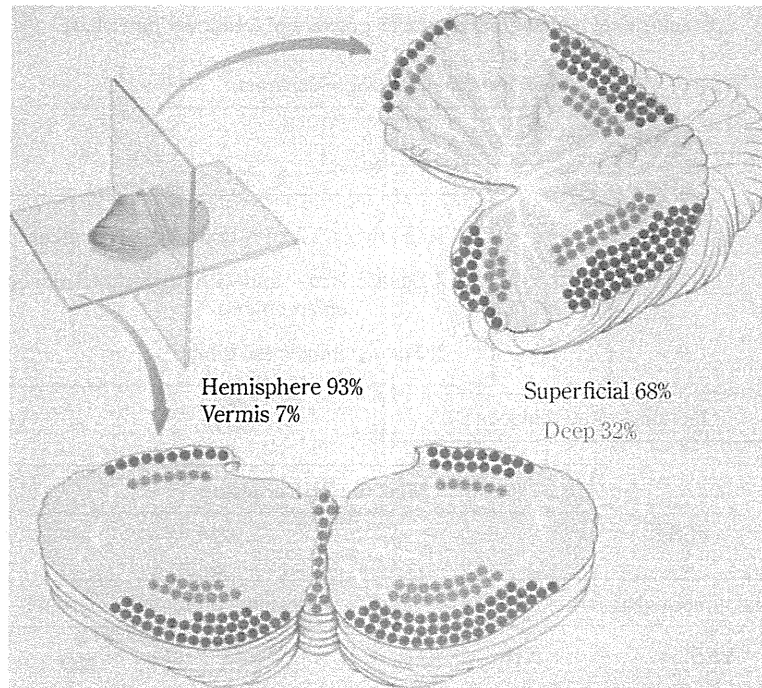
Fig. 7 Localization of cerebellar hemagioblastoma
Blot indicates the tumor locating at superficial position of hemisphere,
deep position of hemisphere, and vermis. (Reprinted with permission from
Ref. 7)

Table 2 Sterotactic radiotherapy for craniospinal hemangioblastomas associated with VHL disease

Authors	Modality	No. of Pts.	No. of tumors	Mean follow-up (ys.)	Control rate (%)	Ref.
Page et al (1993)	LINAC	4	11	>1.5 (0.6~2.5)	100	(15)
Chang et al (1998)	LINAC	13	29	3.6 (0.9~7)	97	(4)
Rajaraman et al (2004)	GK	13	27	2.8 (0.6~6.6)	83	(18)
Moss et al (2009)	LINAC/CK	31 (26) *	92	5.8 (0.4~13.6)	85 (3 yr.) 82 (5 yr.)	(14)
Asthagiri et al (2010)	LINAC/GK	20	44	8.5 (3~17.6)	91 (2 yr.) 51 (15 yr.)	(2)

LINAC : linear accelerator, CK : CyberKnife, GK : gamma-knife
*31 cases were reported, among them 26 of 31 were the patients with VHL disease were 26 cases.

(from the report by Asthagiri[2])

関しては改善 8 手術, 変化なし 34 手術, 悪化 9 手術という結果であった. しかし悪化した 9 手術も半年後には術前の神経学的なレベルまで改善しており, 手術は安全に施行できている. 彼らは予後因子として腫瘍と囊胞のサイズを挙げており, 局在は関係なく, さらには延髄空洞症の存在は術後の神経症状改善に寄与すると報告している. 脊髄の血管芽腫の手術による治療成績も同じグループより報告されているが, 脊髄の血管芽腫も脳幹の

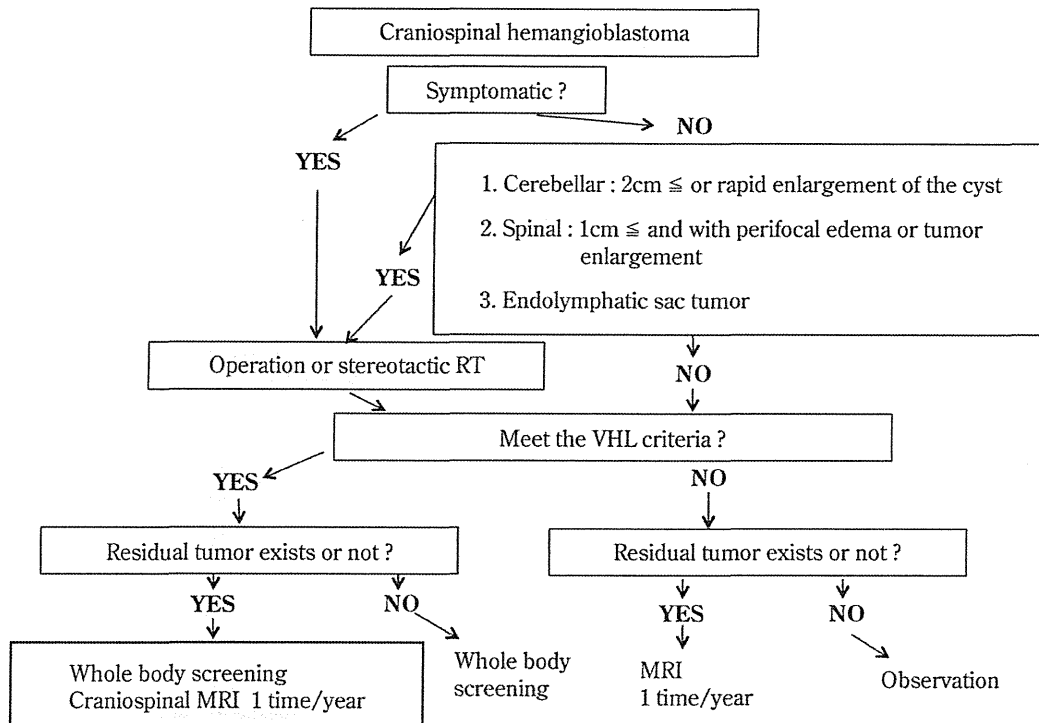Craniospinal hemangioblastoma diagnosis and treatment flow chart

Fig. 8　**Flow chart of the diagnosis and therapeutic dicision**（Reprinted with permission from Ref. 21）

血管芽腫と同様に背側にできることが多い．Mehta ら[13] は 108 症例（156 手術，218 病変）の手術成績を報告しているが，217 病変（99.5％）において腫瘍は全摘出されている．術後平均観察期間 7±5 年と長期フォローしているが，術後 6 カ月後の治療成績の評価は 149 手術（96％）において改善もしくは安定しており，7 手術（4％）にのみ悪化が認められた．症状悪化の要因としては腫瘍の局在が最も関係しており，腹側の病変もしくは完全に脊髄内に存在する病変に関しては注意を要する．長期フォローでも比較的安定しており，10～15 年のフォローアップでは 78％の症例は安定しているが，そのほかの症例はむしろほかの VHL 関連病変にて症状悪化をきたしていたとの報告であった．小脳，脳幹，脊髄の血管芽腫の手術成績に関しては，VHL 病ではない S-HB の手術成績と相違ないとしているが，長期的にみると新病変の出現，手術の回数，他臓器の病変などによる差が生じているようである．

② 定位放射線治療

VHL 病に伴う血管芽腫に対する定位放射線治療に関するいくつかの報告があるが，いずれの報告も腫瘍増大の制御には，ある程度効果的としている[2)4)14)15)18)]（Table2）．Moss ら[14]の報告によると，82 病変のうち 13 病変が増大したが，18 病変が縮小し，51 病変が不変であり，3 年および 5 年の腫瘍増大の制御率は 85％および 82％であったと報告している．また，Asthagiri ら[2]が 20 症例（44 病変，39 小脳，5 脳幹）について長期的にフォローアップしているが，2 年，5 年，10 年，15 年の制御率はそれぞれ 91％，83％，61％，51％である．やはり長期間になると腫瘍は増大してくる傾向である．彼らは，血管芽腫における定位放射線治療の適応は，あくまで手術にて摘出困難な腫瘍であり，小さな無症候性の血管芽腫に関しては定位放射線治療は留保すべきとしている．現時点で血管芽腫における定位放射線治療は，手術困難な症例に対する代替的なもしくは palliative な治療の一つとして位置づけられているようである．

新たな治療の試み

VHL 病に伴う血管芽腫は，*VHL* 遺伝子産物の不活化により血管内皮増殖因子（VEGF）が制御できなくなることで腫瘍が形成される．理論的には血管芽腫の増大をコントロールするにあたって血管増殖を抑制する治療（antiangiogenic therapy）は効果的であるはずである．サリドマイド（thalidomide）は，新生血管の造成に抑制的に働くことから血管芽腫の腫瘍増大をコントロールできる可能性を期待され，脊髄の血管芽腫の増大をコントロールできたという報告がある[20]．また，チロシンキナーゼのインヒビターであるスニチニブ（sunitinib）は，VEGFR や PDGFR のリン酸化を抑制し，細胞の増殖を制御することから VHL 病に対する分子標的治療薬として期待され，治験が行われた．その結果腎癌には効果があるが，血管芽腫にはあまり効果がみられなかった[10]．VEGFR の抗体であるベバシズマブ（bevacizumab）も長期投与により網膜の血管芽腫に効果的であったとの報告もあるが[6]，中枢神経系の血管芽腫における報告はされていない．現時点で，中枢神経系の血管芽腫の治療において手術による治療成績を超える薬剤は見出されていないが，多数の分子標的薬剤が臨床応用されてきている現在，血管芽腫に対する特異的な分子標的治療薬の開発も期待できる．

診断治療のチャート

中枢神経系血管芽腫の診断および治療方針についてのフローチャートに関しては，執印らがガイドラインの中で提示している[21]（Fig. 8）．まず，症候性かどうかにて治療適応を決定し，VHL 病の診断基準を満たせば，全身スクリーニングまで行う必要があるとしており，中枢神経系の血管芽腫に関しては病変があれば，最低 1 年に 1 度の MRI 検査を推奨している．

まとめ

VHL 病に伴う中枢神経系血管芽腫は一生涯で多発し，また再発を繰り返す．特発性の血管芽腫より若年発症で多発性であることが特徴であり，度重なる手術，またほかの全身性疾患の合併もあることにより，患者の QOL は低く，決して予後良好な疾患ではないと考えられる．遺伝性疾患でもあり，カウンセリング等も必要な場合もある．ほかの臓器の病変に関しては専門医と相談しながら，トータルケアを行えば，比較的 QOL を高く保ちな

がら長期生存を望める場合も少なくない．診断，治療のタイミングを誤ってはならない疾患である．

文 献

1) Ammerman JM, Lonser RR, Dambrosia J, Butman JA, Oldfield EH：Long-term natural history of hemangioblastomas in patients with von Hippel-Lindau disease：implications for treatment. *J Neurosurg* **105**：248-255, 2006.

2) Asthagiri AR, Mehta GU, Zach L, Li X, Butman JA, Camphausen KA, Lonser RR：Prospective evaluation of radiosurgery for hemangioblastomas in von Hippel-Lindau disease. *Neuro Oncol* **12**：80-86, 2010.

3) Beitner MM, Winship I, Drummond KJ：Neurosurgical considerations in von Hippel-Lindau disease. *J Clin Neurosci* **18**：171-180, 2011.

4) Chang SD, Meisel JA, Hancock SL, Martin DP, McManus M, Adler JR Jr：Treatment of hemangioblastomas in von Hippel-Lindau disease with linear accelerator-based radiosurgery. *Neurosurgery* **43**：28-34, 1998.

5) Goto T, Nishi T, Kunitoku N, Yamamoto K, Kitamura I, Takeshima H, Kochi M, Nakazato Y, Kuratsu J, Ushio Y：Suprasellar hemangioblastoma in a patient with von Hippel-Lindau disease confirmed by germline mutation study：case report and review of the literature. *Surg Neurol* **56**：22-26, 2001.

6) Hrisomalos FN, Maturi RK, Pata V：Long-term use of intravitreal bevacizumab (avastin) for the treatment of von hippel-lindau associated retinal hemangioblastomas. *Open Ophthalmol J* **4**：66-69, 2010

7) Jagannathan J, Lonser RR, Smith R, DeVroom HL, Oldfield EH：Surgical management of cerebellar hemangioblastomas in patients with von Hippel-Lindau disease. *J Neurosurg* **108**：210-222, 2008.

8) Jagannathan J, Lonser RR, Smith R, DeVroom HL, Oldfield EH：Surgical management of cerebellar hemangioblastomas in patients with von Hippel-Lindau disease. *J Neurosurg* **108**：210-222, 2008.

9) Jarrell ST, Vortmeyer AO, Linehan WM, Oldfield EH, Lonser RR：Metastases to hemangioblastomas in von Hippel-Lindau disease. *J Neurosurg* **105**：256-263, 2006.

10) Jonasch E, McCutcheon IE, Waguespack SG, Wen S, Davis DW, Smith LA, Tannir NM, Gombos DS, Fuller GN, Matin SF：Pilot trial of sunitinib therapy in patients with von Hippel-Lindau disease. *Ann Oncol* **22**：2661-2666, 2011.

11) Lonser RR, Butman JA, Kiringoda R, Song D, Oldfield EH：Pituitary stalk hemangioblastomas in von Hippel-Lindau disease. *J Neurosurg* **110**：350-353, 2009.

12) Lonser RR, Glenn GM, Walther M, Chew EY, Libutti SK, Linehan WM, Oldfield EH：von Hippel-Lindau disease. *Lancet* **361**：2059-2067, 2003.

13) Mehta GU, Asthagiri AR, Bakhtian KD, Auh S, Oldfield EH, Lonser RR：Functional outcome after resection of spinal cord hemangioblastomas associated with von Hippel-Lindau disease. *J Neurosurg Spine* **12**：233-242, 2010.

14) Moss JM, Choi CY, Adler JR Jr, Soltys SG, Gibbs IC, Chang SD：Stereotactic radiosurgical treatment of cranial and spinal hemangioblastomas. *Neurosurgery* **65**：79-85, 2009.

15) Page KA, Wayson K, Steinberg GK, Adler JR Jr：Stereotaxic radiosurgical ablation：an alternative treatment for

recurrent and multifocal hemangioblastomas. A report of four cases. *Surg Neurol* **40**：424-428, 1993.

16) Pavesi G, Berlucchi S, Munari M, Manara R, Scienza R, Opocher G：Clinical and surgical features of lower brain stem hemangioblastomas in von Hippel-Lindau disease. *Acta Neurochir* **152**：287-292, 2010.

17) Peyre M, David P, Van Effenterre R, François P, Thys M, Emery E, Redondo A, Decq P, Aghakhani N, Parker F, Tadié M, Lacroix C, Bhangoo R, Giraud S, Richard S：Natural history of supratentorial hemangioblastomas in von Hippel-Lindau disease. *Neurosurgery* **67**：577-587, 2010.

18) Rajaraman C, Rowe JG, Walton L, Malik I, Radatz M, Kemeny AA：Treatment options for von Hippel-Lindau's haemangioblastomatosis：the role of gamma knife stereotactic radiosurgery. *Br J Neurosurg* **18**：338-342, 2004.

19) Rivera AL, Takei H, Zhai J, Shen SS, Ro JY, Powell SZ：Useful immunohistochemical markers in differentiating hemangioblastoma versus metastatic renal cell carcinoma. *Neuropathology* **30**：580-585, 2010.

20) Sardi I, Sanzo M, Giordano F, Buccoliero AM, Mussa F, Aricò M, Genitori L：Monotherapy with thalidomide for treatment of spinal cord hemangioblastomas in a patient with von Hippel-Lindau disease. *Pediatr Blood Cancer* **53**：464-467, 2009.

21) 執印太郎：フォン・ヒッペル・リンドウ（VHL）病診療ガイドライン．東京，中外医学社，2011.

22) Wanebo JE, Lonser RR, Glenn GM, Oldfield EH：The natural history of hemangioblastomas of the central nervous system in patients with von Hippel-Lindau disease. *J Neurosurg* **98**：82-94, 2003.

23) Wanebo JE, Lonser RR, Glenn GM, Oldfield EH：The natural history of hemangioblastomas of the central nerbous system in patients with von Hippel-Lindau disease. *J Neurosurg* **98**：82-94, 2003.

24) Weil RJ, Lonser RR, DeVroom HL, Wanebo JE, Oldfield EH：Surgical management of brainstem hemangioblastomas in patients with von Hippel-Lindau disease. *J Neurosurg* **98**：95-105, 2003.

25) Weinbreck N, Marie B, Bressenot A, Montagne K, Joud A, Baumann C, Klein O, Vignaud JM：Immunohistochemical markers to distinguish between hemangioblastoma and metastatic clear-cell renal cell carcinoma in the brain：utility of aquaporin1 combined with cytokeratin AE1/AE3 immunostaining. *Am J Surg Pathol* **32**：1051-1059, 2008.

26) Wind JJ, Bakhtian KD, Sweet JA, Mehta GU, Thawani JP, Asthagiri AR, Oldfield EH, Lonser RR：Long-term outcome after resection of brainstem hemangioblastomas in von Hippel-Lindau disease. *J Neurosurg* **114**：1312-1318, 2011.

──────── 要　旨 ────────

VHL 病に伴う中枢神経系血管芽腫

中村　英夫　　倉津　純一　　執印　太郎

　Von Hippel-Lindau（VHL）病は中枢神経系に血管芽腫が発生するだけでなく，全身性に嚢胞や腫瘍が認められる疾患であり，神経線維腫症と並んで脳神経外科医が携わる代表的な遺伝病である．常染色体優性遺伝の形式をとり，浸透率がほぼ 100%である VHL 病は 3 番染色体上の腫瘍抑制遺伝子である *VHL* 遺伝子の異常が原因で起こるということが 1993 年に報告された．それ以来，*VHL* 遺伝子にて翻訳されるタンパク質のさまざまな機能が解明された．最も代表的な機能としては，hypoxia inducible factor（HIF）-1αの制御であり，正常酸素圧において水酸化を受けた HIF-1αをユビキチン化酵素である VHL タンパクが認識し，いくつかのタンパク質と共同して分解する．HIF-1αは転写因子であり vascular endothelial growth factor（VEGF）などの発現を誘導するために，VHL タンパクの機能異常が起こると，血管新生が制御されなくなることが血管芽腫の発生にかかわると考えられている．VHL 病はほかの臓器にも嚢胞や腫瘍が形成されるために，その診断，治療において他科と協力して行う必要がある．その治療の適応やタイミング等を考慮するうえで何らかの役に立つように，VHL 病に伴う中枢神経系血管芽腫における最近の治験をレビューする．

──────── 脳外誌　22：52-60, 2013 ────────